Analysis of tumor evasion mechanisms contributing to tumor radio-resistance and the radio-sensitizing effects of Janus kinase inhibitor oclacitinib in canine tumor cell lines

（イヌ腫瘍細胞における放射線治療抵抗性に関わる免疫回避機構の解析および Janus kinase 阻害薬オクラシチニブの放射線増感効果に関する基礎的研究）

Ryo Owaki

CONTENTS

ABBREVIATIONS

APC	allophycocyanin
Bcl-x_L	B-cell lymphoma-extra large
CDK	cyclin-dependent kinase
CSN5	COP9 signalosome 5
CXCL	C-X-C motif chemokine ligand
EGFR	epidermal growth factor receptor
FBS	fetal bovine serum
GAPDH	glyceraldehyde-3-phosphate dehydrogenase
ICD	immunogenic cell death
ICIs	immune checkpoint inhibitors
IFN	interferon
IL	interleukin
IRF1	interferon-responsive factor 1
JAK	Janus kinase
MCL1	myeloid cell leukemia 1
NFKB	nuclear factor kappa B subunit
NF-κB	nuclear factor kappa B
PARP	Poly (ADP-ribose) polymerase
PBS	phosphate-buffered saline
PCR	polymerase chain reaction
PD-1	programmed death 1
PD-L1	programmed death ligand 1
PTGS	prostaglandin-endoperoxide synthase
RELA	RELA proto-oncogene, NF-kB subunit
RELB	RELB proto-oncogene, NF-kB subunit
RNA-seq	RNA-sequencing

RPMI	Roswell Park Memorial Institute medium
RT-qPCR	reverse-transcription quantitative PCR
SD	standard deviation
STAT	signal transducer and activator of transcription
TME	tumor microenvironment
TNF	tumor necrosis factor

NOTES

The contents of chapter I have been published in *Veterinary and Comparative Oncology*.

Owaki R, Deguchi T, Konnai S, Maekawa N, Okagawa T, Hosoya K, Kim S, Sunaga T, and Okumura M. Regulation of programmed death ligand 1 expression by interferon-γ and tumour necrosis factor-α in canine tumour cell lines. Vet Comp Oncol, 21 (2), 279-290, 2023.

PREFACE

Radiation therapy is a proven treatment for cancer patients in both humans and animals. Over recent decades, advancements in diagnostic imaging, treatment planning, and treatment delivery have improved the accuracy and precision of cancer treatment. These developments can deliver high doses to tumor tissue while minimizing damage to surrounding healthy tissue, thereby improving treatment outcomes [Steven *et al*., 2012]. Regardless of these innovations, most patients would experience tumor recurrence and regrowth after radiation therapy, as tumor cells would complex mechanisms of radio-resistance to ensure their survival. Tumor radio-resistance was a major factor contributing to unfavorable prognoses in cancer patients [Efstathiou *et al*., 2012; Nolan *et al*., 2012]. Therefore, it is essential to investigate the mechanisms underlying radio-resistance in tumors, and novel treatment approaches are required to overcome tumor radio-resistance and improve the outcomes of radiation therapy.

Radiation therapy not only triggers DNA damage in cancer cells but also affects the tumor microenvironment (TME), which is composed of complex biological interactions between the tumor and the surrounding stroma [Langley *et al*., 1997; Ren *et al*., 2023]. After radiation, both direct and indirect effects promoted the release of inflammatory cytokines, such as interleukin (IL)-1 and tumor necrosis factor (TNF)-α, leading to immune cell recruitment. Cytotoxic stress, including chemotherapy and radiation therapy, also facilitated an immune response by generating damage-associated molecular patterns and activating their corresponding pattern recognition receptors. These responses led to immunogenic cell death (ICD) in tumor cells, shifting the primary cytokine profile in the TME towards an immunostimulatory profile including IL-1, IL-6, TNF, and interferon (IFN)-γ. Subsequently, dendritic cells were activated and their maturation into efficient antigen-presenting cells was enhanced. These alterations in TME resulted in the recruitment and activation of T cells [Ashrafizadeh *et al*., 2020]. Immunogenic cell death is recognized as a critical factor in initiating an effective antitumor immune response. A phenomenon known as the radiation-dependent abscopal effect, which represents the observation of ICD in clinical cases, exhibited tumor regression occurring beyond the irradiated areas. [Han *et al*., 2005].

Although radiation therapy leads to ICD, some tumors have evolved to escape

from these immune responses. The immune checkpoint molecules could be one of the important mechanisms for tumor immune evasion in cellular immunity. Programmed death 1 (PD-1), one of the immune checkpoint molecules is a co-inhibitory immunoreceptor. The interaction between PD-1 and its ligand, programmed death ligand 1 (PD-L1), led to the reduction in cytokine production and the suppression of the proliferation of $CD4^+$ and $CD8^+$ T cells [Carter *et al*., 2002]. In cellular immunity, the PD-1/PD-L1 axis would restrain the excessive activation of immune cells.

In contrast, cancer cells utilize the axis to escape the immune responses by binding PD-L1 on the surface of cancer cells to PD-1 on tumor-infiltrating lymphocytes in the TME [Yi *et al*., 2021]. Cumulative studies have reported that PD-L1 was highly expressed in various human cancer cells such as lung carcinoma, melanoma, ovarian adenocarcinoma, and squamous cell carcinoma [Dong *et al*., 2002; Scott *et al*., 2003]. It has been also reported that PD-L1 overexpression was associated with poor treatment outcomes and prognosis of radiation therapy in several types of human tumors, including bladder cancer and esophageal squamous cell carcinoma [Chen *et al*., 2016; Wu *et al*., 2016]. The blockade of the PD-1/PD-L1 axis after irradiation enhanced the effect of irradiation and then induced abscopal effects through the expansion of functional $CD8^+$ T cells in a mouse study [Wei *et al*., 2021]. Immune checkpoint inhibitors (ICIs), including anti-PD-1 antibodies and PD-L1 antibodies, have been developed in humans. Previous studies have demonstrated the efficacy of these antibodies in various types of cancers, including melanoma, renal cell cancer, ovarian cancer, and non-small-cell lung cancer [Brahmer *et al.*, 2012; Hamid *et al.*, 2013], suggesting that ICIs emerged as highly promising treatment options. Recent studies have shown that anti-PD-1 antibodies enhanced local and systemic antitumor effects of radiation therapy through the increase of activated $CD8^+$ T cells in TME in mice [Katsuki *et al.*, 2022]. It was also reported that the blockade of the PD-1/PD-L1 axis combined with irradiation highly induced the abscopal effect [Park *et al.*, 2015]. Moreover, anti-PD-L1 antibody treatment following radiation therapy significantly improved the treatment outcomes compared to radiation therapy alone in non-small-cell lung cancer [Antonia *et al*., 2018]. Another study reported that a combination treatment of radiation therapy and anti-PD-1 antibodies improved the objective response rate at the metastatic site when compared to the treatment with anti-PD-1 antibodies alone in non-small-cell lung cancer [Theelen *et al.*, 2019].

In veterinary fields, PD-L1 overexpression was also reported in various tumors [Maekawa *et al.*, 2023]. Anti-PD-1 antibodies and anti-PD-L1 antibodies have been established, and these antitumor efficacies were demonstrated in various canine tumors, including malignant melanoma, nasal adenocarcinoma, and osteosarcoma [Maekawa *et al.*, 2017; Igase *et al.*, 2020; Maekawa *et al.*, 2023]. The ORR of these antibodies was approximately 20%, which is equivalent to those of humans [Brahmer *et al*, 2012; Hamid *et al*, 2013]. In addition, it was reported that the clinical benefit rate at metastatic sites and the overall survival in dogs treated with anti-PD-L1 antibodies following hypofractionated radiation therapy were higher than those in dogs treated with anti-PD-L1 antibodies alone and dogs receiving concurrent treatment of anti-PD-L1 antibodies and hypofractionated radiation therapy [Deguchi *et al*, 2023]. Therefore, radiation therapy combined with the blockade of the PD-1/PD-L1 axis can be an effective treatment approach. Meanwhile, various mechanisms of resistance to ICIs have been proposed, including those linked to regulatory mechanisms of PD-L1 expression [Iwai *et al*, 2017; Sharma *et al*., 2017], but the regulatory mechanisms of PD-L1 expression on the surface of canine tumor cells remains unclear [Maekawa *et al*., 2017]. Analyzing the regulatory mechanisms of PD-L1 expression is crucial, as it provides opportunities to detect novel therapeutic targets and enhance the effectiveness of PD-1/PD-L1-targeted therapies.

Radiation therapy is a well-documented trigger of PD-L1 expression through both direct DNA damage signaling and inflammatory signaling mechanisms in humans. It has been reported that the ataxia telangiectasia-mutated-checkpoint kinase signaling, which is activated by DNA damage repair, upregulated the signal transducer and activator of transcription (STAT)-interferon regulatory factor 1 (IRF1) signaling pathway and contributed to PD-L1 expression [Sato *et al*., 2017]. In addition, PD-L1 expression was regulated by multiple inflammatory signaling such as IFN-γ, TNF-α, and IL-6 [Moon *et al*., 2017; Wang *et al*., 2017; Xu *et al*., 2018]. Of these, IFN-γ is the outstanding stimulator contributing to the inducible PD-L1 expression through the Janus kinase (JAK)-STAT signaling pathway [Moon *et al*., 2017]. Hence, the JAK-STAT signaling pathway could play a key role in radiation-induced upregulation of PD-L1 expression.

The JAK-STAT signaling pathway is composed of ligand-receptor complexes and 4 members of JAK family (JAK1, JAK2, JAK3, and TYK2) [Krolewski *et al*., 1990; Wilks *et al*., 1991] and 7 members of STAT family (STAT1, STAT2, STAT3, STAT4,

STAT5a, STAT5b, and STAT6) [Shuai *et al*., 1993; Hou *et al*., 1994; Zhong *et al*., 1994; Liu *et al*., 1995]. The STAT family became activated through the phosphorylation of tyrosine residues on the catalytic domain of the receptor by the JAK family. This activation led to the formation of homodimers or heterodimers through SH2-phosphotyrosyl interactions. Subsequently, dimerized STATs translocated into the nucleus, where they bound to DNA-binding sites and regulated the transcription of specific target genes. [Shuai *et al*., 1994]. Numerous essential cellular functions, including hematopoiesis, immune response, tissue repair, apoptosis, and cell proliferation were regulated by STATs [Liu *et al*., 1997; Stephanou *et al*., 2000].

Oclacitinib is an orally available JAK inhibitor for canine dermatitis [Cosgrove *et al*., 2015]. At the recommended clinical doses for canine dermatitis, Oclacitinib demonstrated a preference for inhibiting JAK1 over JAK2, which led to the suppression of JAK1-dependent cytokines related to allergy and inflammation, including IL-2, IL-4, IL-6, and IL-13. Meanwhile, it had minimal impact on JAK2-dependent cytokines associated with hematopoiesis, such as granulocyte-macrophage colony-stimulating factor and erythropoietin, as observed in cellular assays [Gonzales *et al*., 2014]. It was demonstrated that oclacitinib could safely be used for the long-term in dogs [Cosgrove *et al*., 2015].

Of STATs, various studies have shown persistent STAT3 activation in multiple human cancers and cancer cell lines, contributing to poor prognosis [Diaz *et al*., 2006; Zhang *et al*., 2018]. Its activation occurred due to persistent upstream signaling of STAT3, including Src, epidermal growth factor receptor (EGFR), and JAKs [Garcia *et al*., 2001; Jeong *et al*., 2008; Lo *et al*., 2008]. Of these, dysregulation and activation of JAKs have been widely researched. The activation of STAT3 has an important role in the process of malignant transformation. Previous studies have indicated that STAT3 suppressed the induction of apoptosis via regulating survivin expression in several cancer cell lines of humans [Mora *et al*., 2002]. It was suggested that STAT3 induced DNA damage repair, cell proliferation, and invasion in human glioblastoma cell lines [Zhang *et al*., 2018]. The downregulation of PD-L1 expression by inhibiting the JAK2/STAT3 signaling pathway was demonstrated in several human cancer cell lines [Ikeda *et al*., 2016; Chen *et al*., 2018]. The activation of STAT3 plays a key role in TME. It was reported that lack of STAT3 expression induced the increase of proinflammatory cytokines such as IL-6 and TNF-α,

and Dendritic cell maturation in murine tumor cells [Wang *et al*., 2004]. In veterinary medicine, a high level of STAT3 activation has also been reported in several canine tumor cell lines and tissues such as osteosarcoma and mammary carcinoma [Król *et al*., 2011; Bid *et al*., 2012]. It has been reported that highly STAT3 expression correlated with poor prognosis in canine mammary carcinoma and melanoma [Król *et al*., 2011; Liu *et al*., 2021]. The blockade of STAT3 signaling suppressed tumor angiogenesis and tumor growth in the canine osteosarcoma xenograft mouse model [Bid *et al*., 2012].

Recently, it has been reported that irradiation to cells induced further activation of STAT3 in various types of human cancer cell lines, including esophageal carcinoma, pulmonary lung cancer, and prostate cancer [Singh-Gupta *et al*., 2009; Li *et al*., 2013; Wang *et al*., 2022]. The activation of STAT3 in these cell lines enhanced tumor invasiveness, angiogenesis, DNA damage repair. In contrast, several studies demonstrated that a combination treatment of irradiation and JAK or STAT3 inhibitor suppressed STAT3 activation and enhanced radio-sensitivity in tumor xenograft mouse models through several mechanisms, including increase of apoptosis induction, inhibition of PD-L1 expression, and suppression of cell cycle progression [Sun *et al*., 2011; Yan *et al*., 2013]. Therefore, inhibiting the JAK-STAT3 signaling pathway could potentially serve as a therapeutic target to overcome tumor radio-resistance, and oclacitinib may be a promising candidate for an effective treatment for canine tumors with high expression of STAT3 activation, but limited information was available on the antitumor effects of oclacitinib [Barrett *et al*., 2019]. The evaluation of the radio-sensitizing effects of oclacitinib may contribute to the establishment of treatment targeting the JAK-STAT signaling pathway for overcoming the tumor radio-resistance.

The objectives of the present study were to elucidate the mechanisms of tumor radio-resistance focusing on the PD-L1 expression and the JAK-STAT signaling pathway in canine tumors, and to investigate the radio-sensitizing effects of oclacitinib for the establishment of novel therapeutic strategies to overcome tumor radio-resistance. In Chapter I, the effects of proinflammatory cytokines, IFN-γ and TNF-α were examined to demonstrate the upregulation mechanism of PD-L1 expression by these cytokines in canine malignant melanoma cell lines and an osteosarcoma cell line. In Chapter II, radio-sensitizing effects of oclacitinib were evaluated both *in vitro* and *in vivo* using a canine osteosarcoma cell line and a canine malignant melanoma cell line. Furthermore, the

mechanisms underlying the radio-sensitizing effects of oclacitinib were investigated by focusing on the STAT3 signaling pathway. Here this study demonstrates the mechanisms behind tumor radio-resistance with a particular emphasis on the PD-L1 expression and JAK-STAT signaling pathway, providing an opportunity to develop therapeutic agents targeting the JAK-STAT signaling pathway, including oclacitinib.

CHAPTER I

Regulation of programmed death ligand 1 expression by interferon-γ and tumor necrosis factor-α in canine tumor cell lines

INTRODUCTION

In some canine cancer patients, conventional therapies (e.g., surgery, chemotherapy, and radiation therapy) are effective; however, in other patients, tumor growth recurrence and metastasis are problem, and additional or alternative treatments are required. In human medicine, immunotherapies have become available as a novel cancer therapy. Among them, ICIs, such as anti-PD-1 and anti-PD-L1 antibodies, emerged as one of the most promising treatments [Brahmer *et al.*, 2012; Hamid *et al.*, 2013].

Programmed death 1 is an inhibitory receptor expressed on the surface of thymocytes, $CD4^+$ T cells, $CD8^+$ T cells, natural killer cells, and activated monocytes [Nishimura and Honjo, 2001]. Binding of PD-1 to its ligand, PD-L1, which is expressed in a wide range of murine and human cells, results in the downregulation of cytokine production and inhibition of proliferation of $CD4^+$ and $CD8^+$ T cells [Nishimura and Honjo, 2001]. Previous studies have shown that PD-L1 is also expressed on the surface of various human tumor cells, including lung carcinoma, squamous cell carcinoma, and melanoma [Dong *et al*., 2002; Scott *et al*., 2003]. The interaction of PD-1 with PD-L1 in the TME contributes to an immune evasion mechanism for tumor cells by inducing cytotoxic T cell exhaustion [Blank *et al*., 2005]. Indeed, PD-L1 expression on tumor cells is negatively correlated with prognosis and patient survival in several tumors[Hino *et al*., 2010; Muenst *et al*., 2014]. In particular, the activation of cellular immunity is considered one of the antitumor mechanisms in radiation therapy, while tumor immune evasion contributes to tumor radio-resistance [Chen *et al*., 2016; Wu *et al*., 2016]. Many studies on PD-1/PD-L1-targeted immunotherapy have been conducted for antitumor in the last decade, and anti-PD-1/PD-L1 antibodies are now available to be used for antitumor intervention [Hamid *et al*., 2013]. Anti-PD-L1 antibodies and anti-PD-1 antibodies have also been established as treatments in dogs, and pilot studies have suggested the antitumor efficacy against canine tumors, but the ORR of treatment with anti-PD-L1 antibodies and anti-PD-1 antibodies against canine tumors was only 22.2% and 16.7%, respectively. [Maekawa *et al*., 2017; Igase *et al*., 2020]

In human medicine, several resistant mechanisms to ICIs have been suggested, including those associated with the regulation of PD-L1 expression [Sharma *et al*., 2017].

It has been reported that PD-L1 was also expressed on canine tumor cell lines and tissues [Maekawa *et al*., 2014, 2016], however, the regulatory mechanism of PD-L1 expression on canine tumor cells remains largely unclear. Analysis of the regulatory mechanism is of great importance because it will offer opportunities to discover novel therapeutic targets and enhance the effectiveness of PD-1/PD-L1-targeted immunotherapies.

In TME, various regulatory mechanisms of PD-L1 expression (e.g., genomic alterations; epigenetic, transcriptional, and post-transcriptional regulation; and post-translational modification) have been reported in human tumor cells. Among these mechanisms, inflammatory signaling, a transcriptional regulatory mechanism of PD-L1 expression, would play a key role in PD-L1 upregulation [Yi *et al*., 2021]. Proinflammatory cytokines, such as IFN-γ, TNF-α, IL-6, IL-17, and transforming growth factor-β, upregulated PD-L1 expression in human tumor cells [Ni *et al*., 2012; Garcia-Diaz *et al*., 2017; Wang *et al*., 2017]. In particular, IFN-γ would be considered the prominent inducer of PD-L1 [Maekawa *et al*., 2016]. It induced PD-L1 upregulation via the JAK-STAT pathway in a human melanoma cell line [Garcia-Diaz *et al*., 2017]. Specifically, IFN-γ would bind to type II IFN receptor, thereby activating the JAK-STAT signaling pathway and subsequently inducing IRF-1, which ultimately promoted PD-L1 transcription [Schroder *et al*., 2004; Garcia-Diaz *et al*., 2017]. Another cytokine, TNF-α, was also a regulator of PD-L1 expression. It induced PD-L1 upregulation via the nuclear factor kappa B (NF-κB) signaling pathway in human prostate cancer and colon cancer cell lines; upon TNF-α binding to TNF receptor on cancer cells, nuclear translocation of p65 (also known as RELA; a NF-κB family protein) was induced by the removal of IκB kinase from the inactivated NF-κB complex, after which PD-L1 transcription was promoted by p65 through its binding to the PD-L1 promoter [Wang *et al*., 2017; Antonangeli *et al*., 2020]. TNF-α also induced PD-L1 expression at the post-translational level in a human breast cancer cell line; after p65 nuclear translocation, COP9 signalosome 5 (CSN5; the fifth component of the CSN complex with deubiquitination activity) expression was upregulated, and CSN5 inhibits the ubiquitination and subsequent degradation of PD-L1 protein, thereby stabilizing PD-L1 expression on the surface of tumor cells [Lim *et al*., 2016]. In addition to inflammatory signaling, it was reported that DNA damage signaling by X-irradiation upregulated PD-L1 expression on

human osteosarcoma, lung cancer, and prostate cancer cell lines through the STAT-IRF1 pathway [Sato *et al*., 2017].

In this chapter of the study, the regulatory mechanism of PD-L1 expression was investigated in canine tumor cells by assessing PD-L1 expression on tumor cell lines after stimulation with IFN-γ, TNF-α, and X-irradiation. The transcriptomes of the stimulated cell lines were analyzed using RNA-sequencing (RNA-seq) to determine the signaling pathway(s) involved in PD-L1 upregulation following each stimulation. Additionally, the mRNA expression of relevant genes and PD-L1 protein expression were investigated with or without the inhibitor of each signaling pathway to evaluate the contribution of these pathways to PD-L1 expression.

MATEIALS AND METHODS

Cell line validation statement and culture conditions

Two canine malignant melanoma cell lines (CMeC and LMeC) [Inoue *et al*., 2004], and an osteosarcoma cell line (HMPOS) [Barroga *et al*., 1999] were used in this study. Of these, CMeC and LMeC were established in Tokyo University, Japan, and kindly provided by the investigators[Inoue et al., 2004]. HMPOS was established in our laboratory [Barroga *et al*., 1999]. Cell lines were validated to be canine origin by RNA-seq. Cell lines were confirmed to be free of mycoplasma infection using polymerase chain reaction (PCR) at ICLAS Monitoring Center (Kanagawa, Japan). In the present study, these cell lines were cultured in Roswell Park Memorial Institute medium (RPMI) 1640 (Thermo Fisher Scientific, Waltham, MA, USA) supplemented with 10% fetal bovine serum (FBS; Sigma-Aldrich, St. Louis, MO, USA), 100 units/ml penicillin G (Wako Pure Chemical Industries, Osaka, Japan), and 100 μg/ml streptomycin (Wako Pure Chemical Industries) and maintained in a humidified atmosphere with 5% CO_2 at 37°C. Each cell line (1.0×10^5 cells/well) was treated with recombinant canine IFN-γ (10 ng/ml, Kingfisher Biotech, Saint Paul, MN, USA), recombinant canine TNF-α (10 ng/ml, Kingfisher Biotech), the JAK inhibitor oclacitinib (2.5 or 5.0 μM, MedChemExpress, Monmouth Junction, NJ, USA), and/or the NF-κB inhibitor BAY 11-7082 (5 or 10 μM, AdipoGen LIFE SCIENCES, San Diego, CA, USA), or exposed to 5 Gy X-irradiation, then incubated for 24 hours. Following these treatments, cells were gently washed three times with phosphate-buffered saline (PBS). Subsequently, cells were collected and cell viability was tested with 0.4% trypan blue solution (Thermo Fisher Scientific) to confirm the cell viability percentage was more than 90% using Countess II automated cell counter (Thermo Fisher Scientific). The expression of PD-L1 protein was analyzed using flow cytometry, whereas gene expression was analyzed using RNA-seq and reverse-transcription quantitative PCR (RT-qPCR).

X-ray irradiation

The XRAD iR-225 X-ray irradiator (Precision X-Ray, North Branford, Connecticut) was used for X-irradiation for cells at a dose rate of 1.37 Gy/minute. It operated at 200 kVp and 15 mA, and a 1.0 mm aluminum filter was applied, all at room

temperature.

Flow cytometry

To detect expression of canine PD-L1 on the cell surface, flow cytometry with rat α-PD-L1 monoclonal antibody 6C11-3A11, established in a previous report [Takeuchi *et al*. 2020], or an isotype-matched control antibody (rat IgG2a, BD Biosciences, Haryana, India) was performed. Briefly, 2×10^5 cells were resuspended and incubated in 10% goat serum (Thermo Fisher Scientific) in PBS at room temperature for 20 minutes to reduce nonspecific binding of antibodies. Cells were then incubated with 10 μg/ml 6C11-3A11 antibody at room temperature for 30 minutes, washed twice with 10% goat serum in PBS, incubated again with allophycocyanin (APC)-conjugated goat antirat immunoglobulin antibody (Beckman Coulter, Brea, CA, USA) at room temperature for 30 minutes, and finally washed twice before the analysis using a BD FACS Verse Flow Cytometer (BD Biosciences).

RNA-seq

Total RNA was extracted from CMeC cells using RNeasy Micro Kit (Qiagen, Hilden, Germany). The RNA quality was determined for each sample using Bioanalyzer (Agilent Technologies, Santa Clara, CA, USA). The RNA integrity number of each sample was >10 (showing intact RNA). Poly(A)+ RNA was purified using a NEBNext Poly(A) mRNA Magnetic Isolation Module (New England Biolabs, Ipswich, MA, USA). Double-stranded cDNA libraries (RNA-seq libraries) were created by the SMARTer Stranded Total RNA Sample Prep Kit (Takara Bio USA, San Jose, CA, USA) and generated using a Nextseq 500 sequencer (Illumina, San Diego, CA, USA) with paired-end reads. The dog reference genome was used to map the obtained reads using STAR. FeatureCounts was used to count the unique reads mapped to annotated genes, and the mapped reads were used to calculate the FPKM values. Differentially expressed genes were identified using DEseq2. All protocols, except for RNA extraction, were performed in DNAFORM (Yokohama, Japan).

RT-qPCR

Total RNA was extracted from cells using TRIZol reagent (Thermo Fisher

Scientific), and total RNA was quantified using spectrophotometry with the wavelength at 260 nm, RNA (500 ng) was reverse-transcribed to cDNA using M-MLV RT kit (Thermo Fisher Scientific) in a 20 µl reaction. Subsequently, duplicate qPCR was performed for each sample using the KAPA SYBR FAST qPCR Master Mix (2×) Kit (KAPA Biosystems, Wilmington, MA, USA). For each sample, 10 µl KAPA master mix, 200 nM specific primers, and 1 µl cDNA were mixed in a total volume of 20 µl. No template controls were performed by adding nuclease-free water. The qPCR conditions were as follows: initial denaturation at 95°C for 2 minutes, 40 cycles of denaturation at 95°C for 15 seconds, annealing at 60°C for 20 seconds, and extension at 72°C for 1 minute. All relative mRNA expressions were normalized against the reference gene, glyceraldehyde-3-phosphate dehydrogenase (GAPDH) [Hartley *et al*., 2017; Li *et al*., 2019; An *et al*., 2020; Eto *et al*., 2021; Sung *et al*., 2022], and quantified using the delta–delta Ct method [Kumar *et al*., 2017]. The sequences of the primers used in the experiments [De Bruin *et al*., 2005; Peters *et al*., 2005; Wilson *et al*., 2008; Vascellari *et al*., 2013; Kumar *et al*., 2017; Lu *et al*., 2017; Li *et al*., 2019; Akaraphutiporn *et al*., 2021] are listed in Table I-1. All primers, except for those for PD-L1, were used in previous canine tumor studies. The primers for PD-L1 were designed using the Primer3plus program (https://www.primer3plus.com/index.html). All primers were designed to detect all transcript variants. The primers for GAPDH, IL6, JAK2, PD-L1, prostaglandin-endoperoxide synthase (PTGS)2, and nuclear factor kappa B subunit (NFKB)1 were designed to span exon-exon junction(s), although the other primers could not be designed to span the junction because the exon structures have not been registered on the National Centre for Biotechnology Information database (https://www.ncbi.nlm.nih.gov/). The qPCR efficiency of these primers was 93-101%. The specificities of the primer pairs were validated by a single melting peak by the melting curve analysis. Additional information on primers used in this study is available in Table I-2.

Immunocytochemistry for identification of NF-κB p65 localization

Each cell line (1.0×10^4 cells) was cultured in 8-well permanox slides (Thermo Fisher Scientific) in 500 µl of RPMI-1640 medium supplemented with 10% FBS. Cells were incubated with 10 ng/ml of recombinant canine TNF-α with or without 10 µM BAY 11-7082 for 24 hours in a humidified atmosphere with 5% CO_2 at 37°C. Cells were then

gently washed three times with PBS and fixed with 4% paraformaldehyde (Wako Pure Chemical Industries) in PBS for 10 minutes at room temperature. Nonspecific antibody binding was blocked by incubation for 30 minutes in 5% normal goat serum (Thermo Fisher Scientific) in PBS. Nuclear factor kappa B p65 rabbit polyclonal antibody (Cell Signaling Technology, Danvers, MA, USA) (1:100) was used as a primary antibody with incubation at 4°C overnight. Subsequently, cells were washed three times and incubated for 90 minutes at room temperature with fluorescein isothiocyanate-conjugated goat anti-rabbit Immunoglobulin G antibody (Thermo Fisher Scientific) (1:1000). Nuclei were stained using Prolong Diamond Antifade Mountant with DAPI (Thermo Fisher Scientific), and cells were visualized using Zeiss LSM 700 confocal laser microscope (Carl Zeiss AG, Oberkochen, Germany). Two hundred cells were counted and the rate of NF-κB nuclear translocation (number of NF-κB p65-positive nuclei/number of total nuclei × 100 [%]) was calculated in three different fields of each slide.

Statistical analysis

All data are presented as mean ± standard deviation (SD). Statistical analysis was performed using GraphPad Prism 9 software (GraphPad Software, San Diego, CA, USA). The Shapiro-Wilk test was performed to determine whether the values were normally distributed. Unpaired, 2-tailed Student's *t*-test was performed to determine statistical significance, set at $p < 0.05$, between two groups, whereas ANOVA followed by Tukey's multiple comparison test was used to analyze data for three or more groups.

Table I-1 Primer pairs used for RT-qPCR

Gene	Forward primer 5'-3'	Reverse primer 5'-3'
CXCL8	ACTTCCAAGCTGGCTGTTGC	GGCCACTGTCAATCACTCTC
GAPDH	CTGAACGGGAAGCTCACTGG	CGATGCCTGCTTCACTACCT
IL6	CTCTCCACAAGCGCCTTCTC	TGAAGTGGCATCATCCTTGG
JAK1	CCCCCATTGATCGTCCACAA	CACATACATCCCCTCCTCGC
JAK2	TAGGGTTTCCTGGTGCTT	TGTTGTCTTGTAGAGGGTCAT
PD-L1 (CD274)	CTATGGCGGTGCTGACTACAAG	ATGACTTCAGCCTCAGGGTAAC
PTGS2	ACCTGATGACTGTCCAACACC	TCCACAATCTCTTTTGAATCAGG
p50 (NFKB1)	GATGAGATCTTCCTGCTCTGTG	AATGGCTACTTGTCGGTGTAC
p65 (RELA)	GAAACACTGGAAGCACGAATG	TCCTTTTCCCGATCTGTAAGC
STAT1	CCGACTTCAGACGACAGATAAC	GGAAACGTTCACGCTCTACA
STAT3	GTGGAGAAGGACATCAGCGGTAA	AACTTGGTCTTCAGGTATGGGGC

Table I-2 Primer details for RT-qPCR

Gene (Official gene symbol)	Amplicon length (bp)	Target exons	Linear dynamic range (copies)	qPCR efficiency (%)
CXCL8	172	-	10^2–10^5	98
GAPDH	129	8-10	10^2–10^5	94
IL6	102	1-2	10^3–10^6	99
JAK1	108	-	10–10^5	101
JAK2	135	13-14	10–10^5	101
PD-L1 (CD274)	144	3-4	10^4–10^7	94
PTGS2	72	5-6	10^2–10^6	98
P50 (NFKB1)	131	7-8	10–10^4	94
p65 (RELA)	123	-	10–10^6	95
STAT1	124	-	10^2–10^5	93
STAT3	260	-	1-10^4	99

RESULTS

Upregulation of PD-L1 expression on tumor cell lines via stimulation with IFN-γ and TNF-α, but not X-irradiation

According to flow cytometry analysis, PD-L1 expression was no significant difference between no treatment control and cells exposed to X-irradiation on all tumor cell lines (CMeC, LMeC, and HMPOS) (Figure I-1). In contrast, IFN-γ and TNF-α significantly increased PD-L1 expression on all cell lines (CMeC, LMeC, and HMPOS) (Figure I-2A-D). The combination of IFN-γ and TNF-α treatment further enhanced PD-L1 expression compared with the effect of either IFN-γ or TNF-α alone (Figure I-2E, F). Thus, PD-L1 expression is seemingly cooperatively regulated by IFN-γ and TNF-α, possibly through distinct mechanisms.

Activation of the JAK-STAT signaling pathway following treatment with IFN-γ

Consistent with flow cytometric analysis, RNA-seq analysis relative to control (untreated) cells showed that *PD-L1* mRNA expression was higher in IFN-γ–treated cells (log_2 fold change: 3.518; Figure I-2A). Moreover, expression of *STAT1* (2.040), *STAT3* (1.501), and genes regulated by STAT activation, namely *interferon induced protein 44* (5.929), *IRF1* (4.010), and *2'-5'-oligoadenylate synthetase 1* (3.034) [Lu *et al*., 2017], was upregulated in CMeC cells treated with IFN-γ (Figure I-3A). To determine the relationship between PD-L1 expression and the JAK-STAT signaling pathway, the cell lines were incubated with IFN-γ and the JAK inhibitor oclacitinib, and the mRNA expression of *JAK1*, *JAK2*, *STAT1*, *STAT3*, *PD-L1*, and the STAT-regulated genes *PTGS2* and *IL6* [Liu *et al*., 2020] was analyzed using RT-qPCR. *JAK1* and *JAK2* expression was upregulated by IFN-γ in LMeC and CMeC cells, respectively, whereas *STAT1* and *STAT3* mRNA expression was increased in all three cell lines. *PD-L1* and *PTGS2* expression were upregulated in all three cell lines upon IFN-γ stimulation, and *IL6* mRNA expression was higher in CMeC and LMeC cells. Expression of all these upregulated genes was suppressed by the addition of oclacitinib, indicating that the JAK-STAT pathway is involved in canine IFN-γ signaling and contributes to *PD-L1* mRNA expression (Figure I-3B).

Activation of the NF-κB signaling pathway following treatment with TNF-α

In CMeC cells, mRNA expression profiles were analyzed using RNA-seq upon TNF-α stimulation. *PD-L1* mRNA expression was not changed by TNF-α stimulation in CMeC ($\log_2$ fold change, −0.214). However, the expression of NF-κB family genes, *RELB proto-oncogene, NF-kB subunit (RELB)* (2.916) and *NFKB2* (2.360), and genes regulated by NF-κB activation, namely *C-X-C motif chemokine ligand (CXCL)8* (4.232) and *PTGS2* (2.273) [Amiri and Richmond, 2005], was upregulated upon TNF-α treatment (Figure I-4A).

To determine the relationship between *PD-L1* expression and the NF-κB signaling pathway, each cell line was incubated with TNF-α and the NF-κB inhibitor BAY 11-7082, and the mRNA expression of *RELA proto-oncogene, NF-kB subunit (RELA)*, *NFKB1*, *PD-L1*, *CXCL8*, and *PTGS2* were analyzed using RT-qPCR. The expression of *RELA* in all three cell lines, and the expression of *NFKB1* in LMeC and HMPOS cells were at a higher level upon TNF-α treatment. Consistent with data for CMeC cells, *PD-L1* expression was upregulated only in LMeC cells upon TNF-α stimulation, whereas *CXCL8* and *PTGS2* expression was higher in all three cell lines. The addition of BAY 11-7082 suppressed the upregulation of all genes, indicating that the NF-κB pathway is involved in canine TNF-α signaling, although its direct contribution to *PD-L1* mRNA expression seems limited (Figure I-4B).

Upon NF-κB activation, the NF-κB complex translocates into the nucleus to promote transcription of its target genes [Hayden and Ghosh, 2008]. To assess NF-κB translocation in canine tumor cell lines upon TNF-α stimulation, NF-κB p65 localization was examined using immunocytochemistry. Without TNF-α stimulation, NF-κB p65 mainly accumulated in the cytoplasm (Figure I-5A); after 24 hours of incubation with TNF-α, NF-κB p65 showed its nuclear translocation in all three cell lines, indicating that NF-κB signaling had been activated (Figure I-5A). BAY 11-7082 suppressed the nuclear translocation of NF-κB p65 (Figure I-5A), confirming its potency as an inhibitor of NF-κB activation. The respective nuclear translocation rates in CMeC, LMeC, and HMPOS cells were as follows: 14.17 ± 1.03%, 30.67 ± 6.01%, and 17.00 ± 6.01% under control conditions; 93.83 ± 2.25%, 93.83 ± 1.65%, and 93.50 ± 0.82% following TNF-α treatment, and 27.33 ± 12.07%, 73.00 ± 6.02%, and 50.12 ± 6.33% following TNF-α and BAY 11-7082 treatment (Figure I-5B).

Effects of oclacitinib and BAY 11-7082 on PD-L1 protein expression

According to flow cytometry analysis, PD-L1 induction by IFN-γ was significantly inhibited by 2.5 or 5.0μM oclacitinib treatment in all cell lines. The extent of inhibition varied according to the concentration of oclacitinib used. The respective PD-L1 expression (MFI) under IFN-γ, IFN-γ and 2.5μM oclacitinib, and IFN-γ and 5.0μM oclacitinib treatment conditions were as follows: 300 ± 73, 148 ± 36, and 72 ± 39 in CMeC cells; 188 ± 29, 122 ± 22, and 99 ± 37 in LMeC cells; and 817 ± 122, 378 ± 92, and 140 ± 64 in HMPOS cells (Figure I-6).

Induction of PD-L1 by TNF-α was also significantly inhibited by 5μM BAY 11-7082 in CMeC cells and by 10μM BAY 11-7082 in all three cell lines. The extent of inhibition varied in a dose-dependent manner. The respective PD-L1 expression (MFI) under TNF-α, TNF-α and 5.0μM BAY 11-7082, and TNF-α and 10μM BAY 11-7082 treatment conditions were as follows: 154 ± 28, 90 ± 19, and 92 ± 6 in CMeC cells; 324 ± 46, 259 ± 50, and 214 ± 42 in LMeC cells; and 112 ± 29, 78 ± 19, and 47 ± 27 in HMPOS cells (Figure I-7).

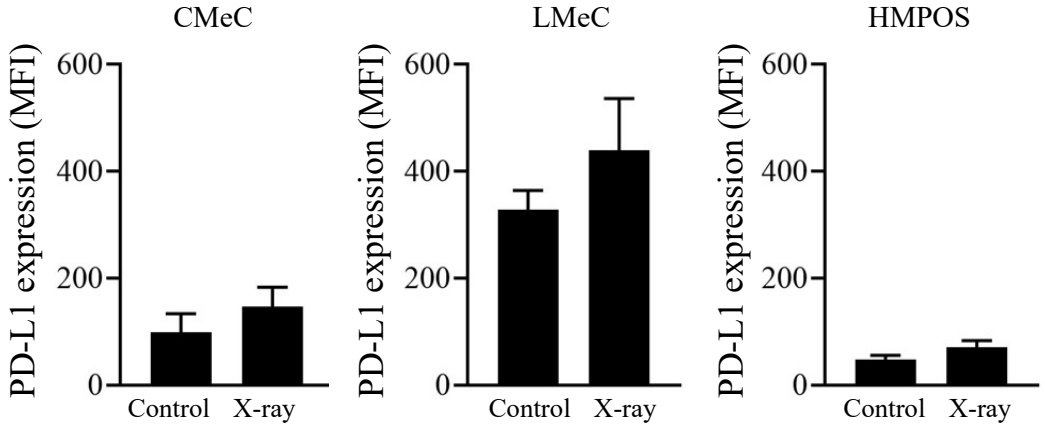

Figure I-1. Induction of PD-L1 expression on canine tumor cell lines after exposure to X-irradiation

PD-L1 expression (MFI) on tumor cells 24 hours after X-irradiation exposure (X-ray).

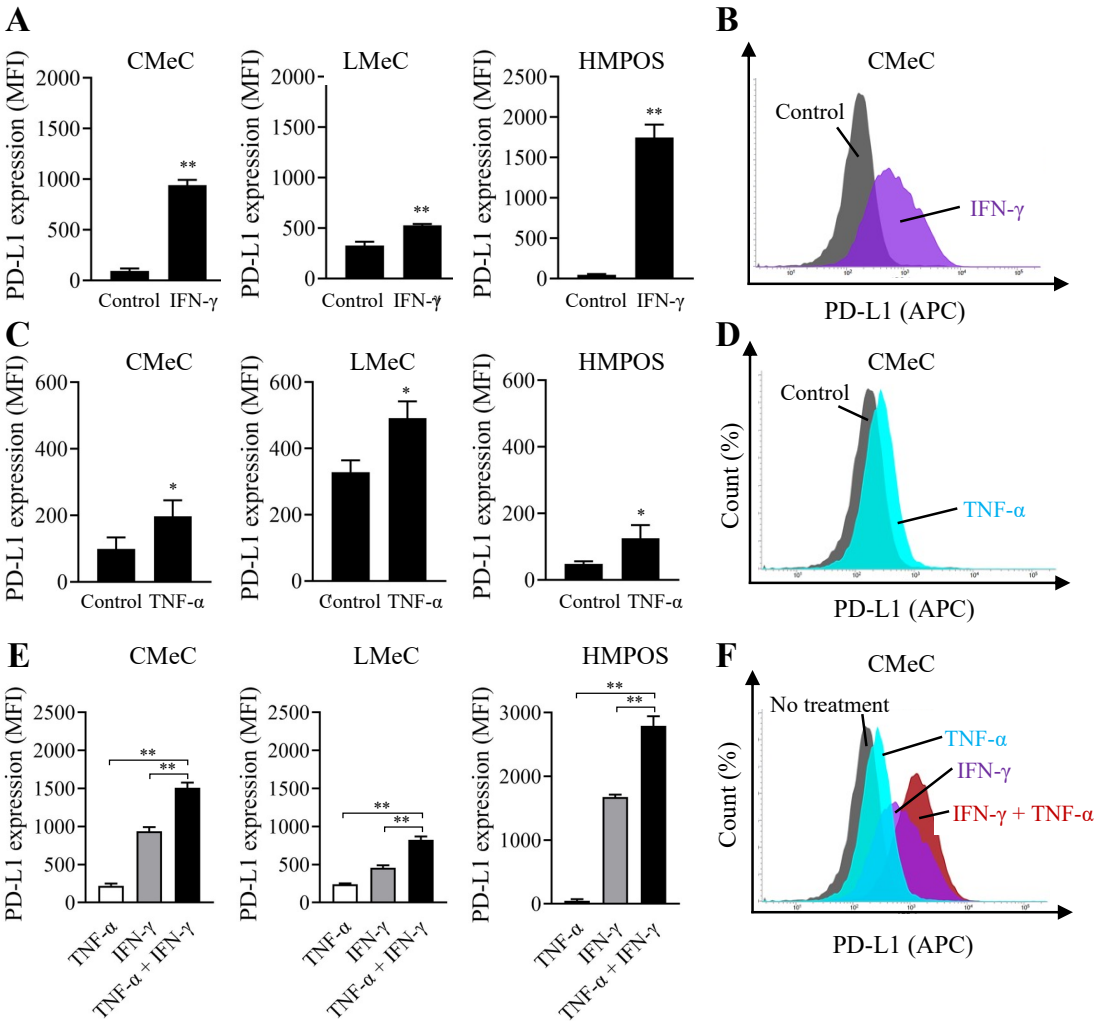

Figure I-2. Induction of PD-L1 expression on canine tumor cell lines treated with IFN-γ and TNF-α

(A) PD-L1 expression (MFI) after tumor cells were incubated with 10 ng/ml IFN-γ for 24 hours. (B) PD-L1 expression on tumor cells treated with IFN-γ. (C) PD-L1 expression (MFI) after tumor cells were incubated with 10 ng/ml TNF-α for 24 hours. (D) PD-L1 expression on tumor cells treated with TNF-α. (E) Effects of an IFN-γ and TNF-α combination treatment on PD-L1 expression on tumor cells. (F) PD-L1 expression on tumor cells incubated with a combination of IFN-γ and TNF-α. Student's *t*-test was used to compare two groups; ANOVA with a post-hoc Tukey's multiple comparison test was used to compare three groups. *$p < 0.05$ and **$p < 0.01$.

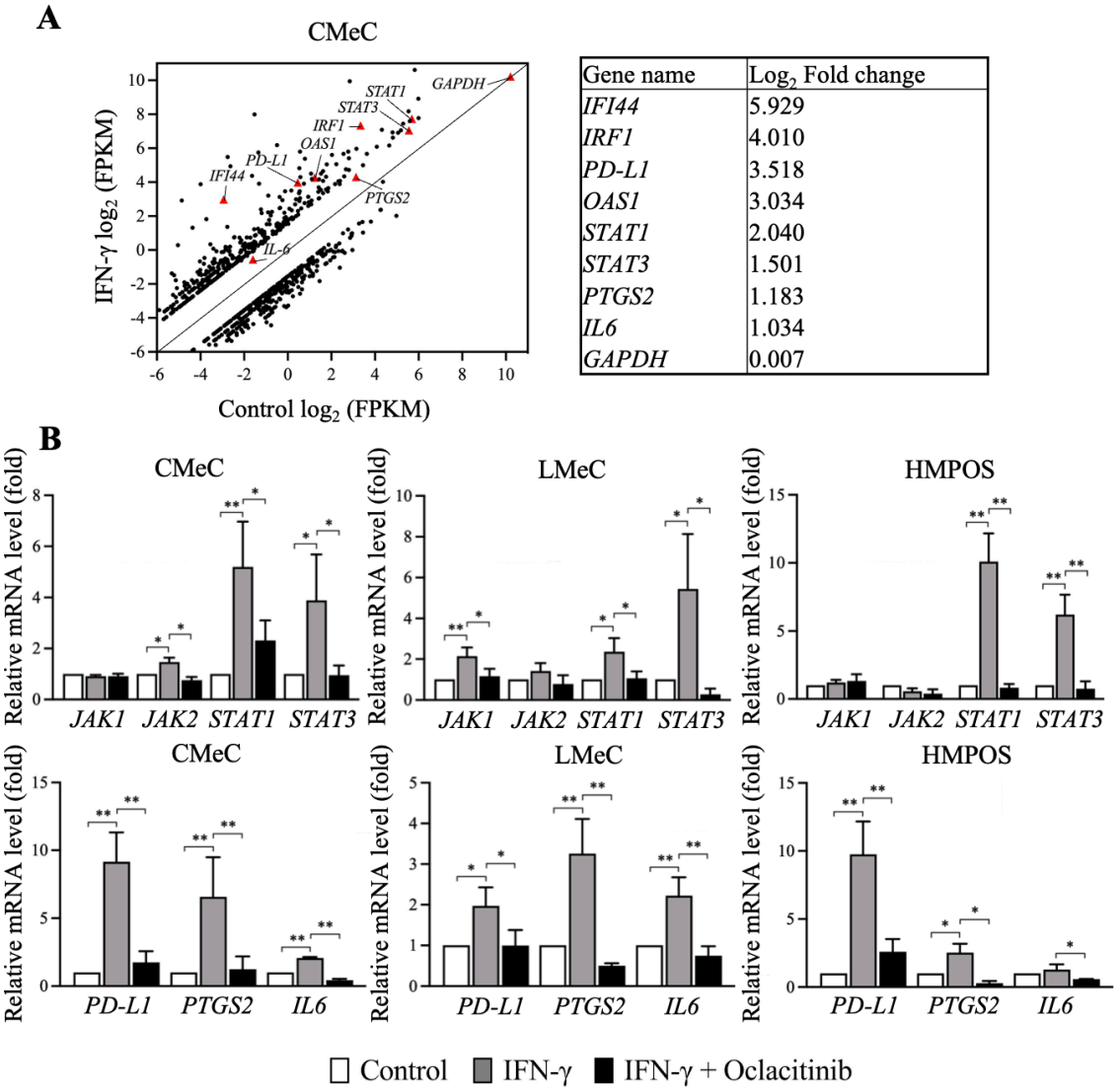

Gene name	Log_2 Fold change
IFI44	5.929
IRF1	4.010
PD-L1	3.518
OAS1	3.034
STAT1	2.040
STAT3	1.501
PTGS2	1.183
IL6	1.034
GAPDH	0.007

Figure I-3. Gene expression in tumor cell lines incubated with IFN-γ

(A) Scatter plot showing the gene expression level of IFN-γ–treated vs. control CMeC cells quantified using RNA-seq. Genes of interest are shown as red triangles. (B) Relative mRNA levels of *JAK1/2*, *STAT1/3*, *PD-L1*, *PTGS2*, and *IL6* quantified using RT-qPCR. ANOVA with a post-hoc Tukey's multiple comparison test was used for statistical analysis. *$p < 0.05$ and **$p < 0.01$.

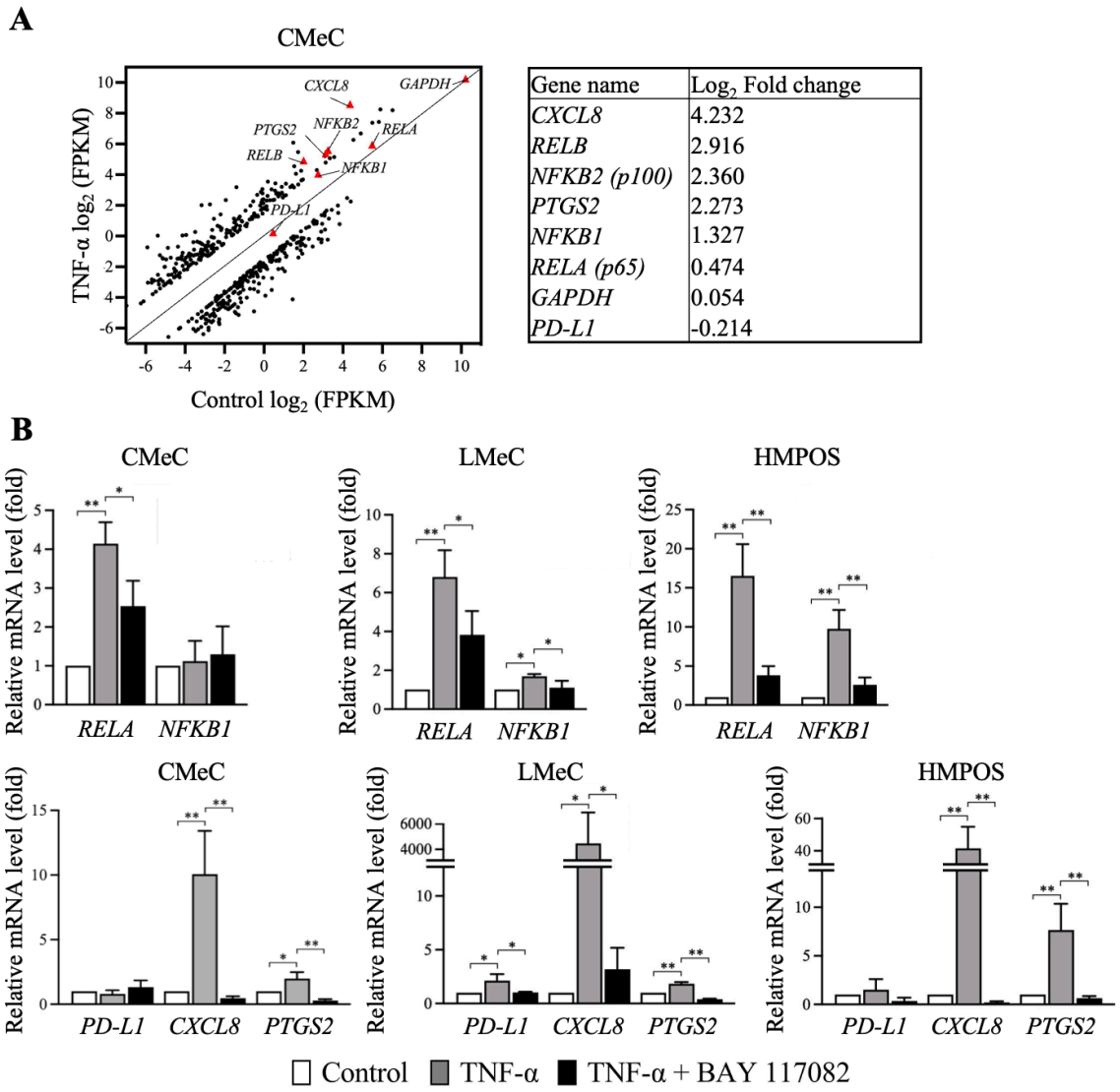

Gene name	Log_2 Fold change
CXCL8	4.232
RELB	2.916
NFKB2 (p100)	2.360
PTGS2	2.273
NFKB1	1.327
RELA (p65)	0.474
GAPDH	0.054
PD-L1	-0.214

Figure I-4. Gene expression in tumor cell lines incubated with TNF-α

(A) Scatter plot showing the gene expression level of TNF-α–treated vs. control CMeC cells quantified using RNA-seq. Genes of interest are shown as red triangles. (B) Relative mRNA levels of *RELA*, *NFKB1*, *PD-L1*, *CXCL8* and *PTGS2* quantified using RT-qPCR. ANOVA with a post-hoc Tukey's multiple comparison test was used for statistical analysis. *$p < 0.05$ and **$p < 0.01$.

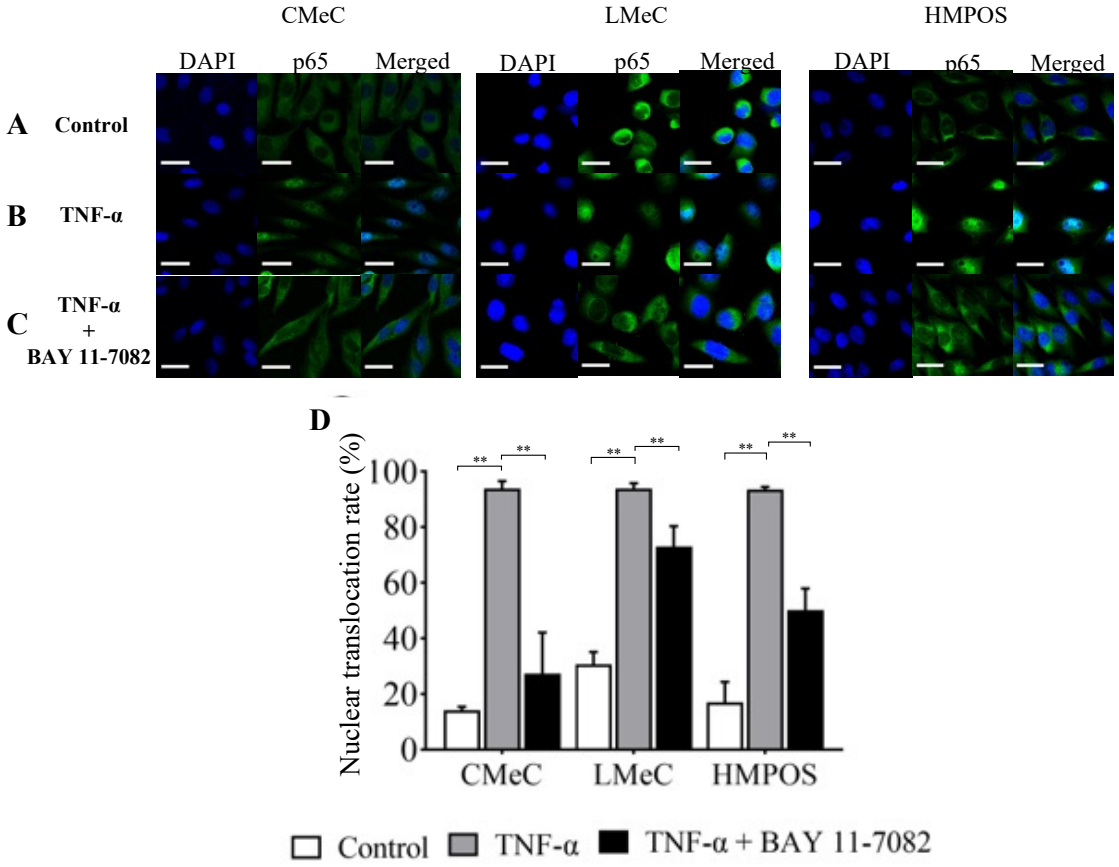

Figure I-5. Decreased NF-κB p65 nuclear translocation in TNF-α–treated tumor cell lines due to the NF-κB inhibitor BAY 11-7082

(A) Immunofluorescence staining of untreated tumor cells showing diffuse cytoplasmic localization of NF-κB p65. (B) Immunofluorescence staining of tumor cells treated with 10 ng/ml of TNF-α showing nuclear translocalization of NF-κB p65. (C) Immunofluorescence staining of tumor cells treated with 10 ng/ml of TNF-α and 10μM BAY 11-7082 showing significant diminution of NF-κB p65 nuclear translocation due to TNF-α stimulation. Scale Bar = 50 μm. (D) Nuclear translocation rate (%, number of NF-κB p65-positive nuclei/number of total nuclei × 100) in each treatment condition. ANOVA with a post-hoc Tukey's multiple comparison test was used for statistical analysis. $^{**}p < 0.01$.

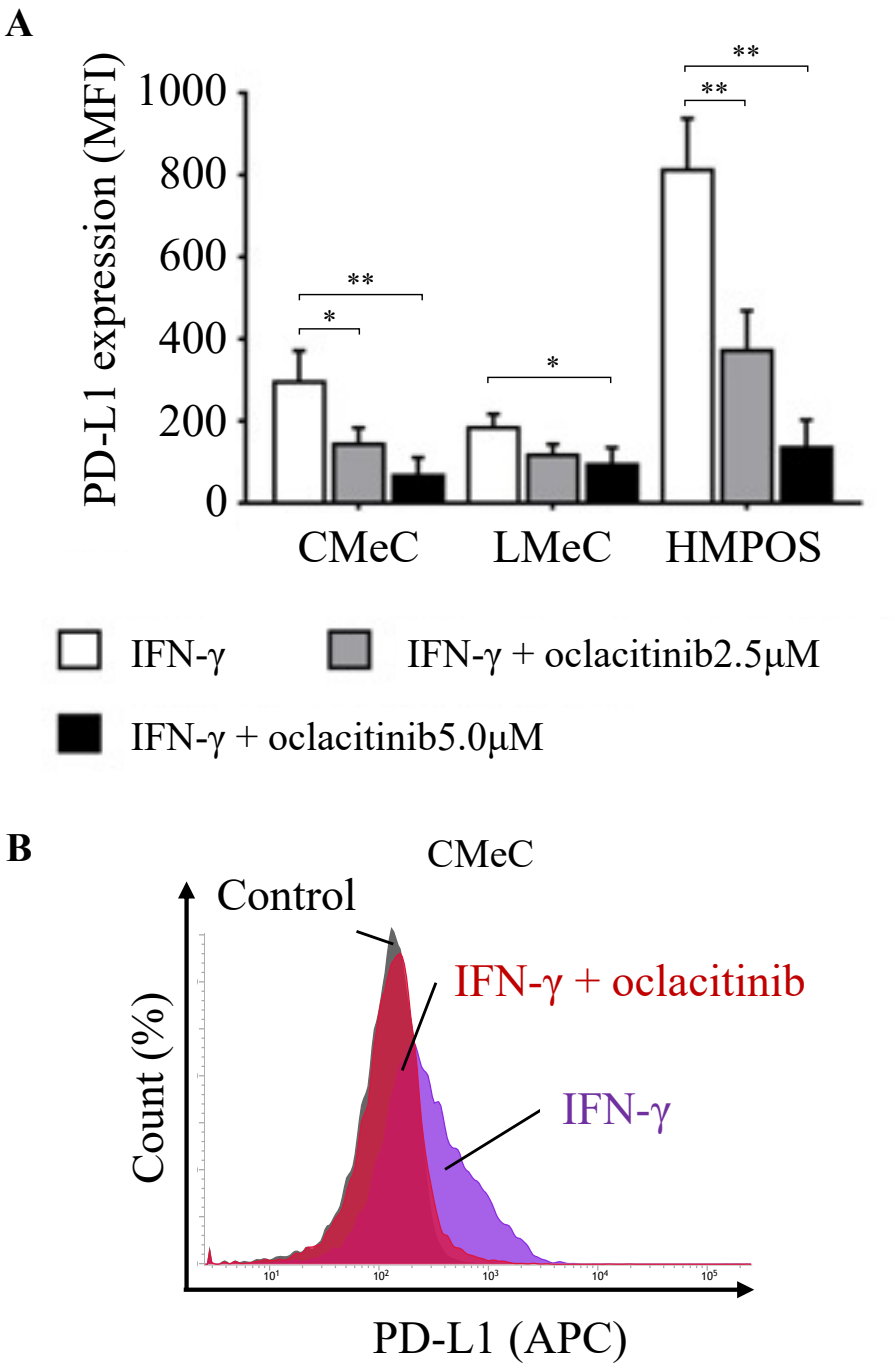

Figure I-6. Inhibition of IFN-γ-induced PD-L1 expression in tumor cells due to the JAK inhibitor oclacitinib

(A) Inhibition of IFN-γ-induced PD-L1 expression due to various concentrations of oclacitinib. (B) PD-L1 expression on tumor cells incubated with IFN-γ and oclacitinib. ANOVA with a post-hoc Tukey's multiple comparison test was used for statistical analysis. *$p < 0.05$ and **$p < 0.01$.

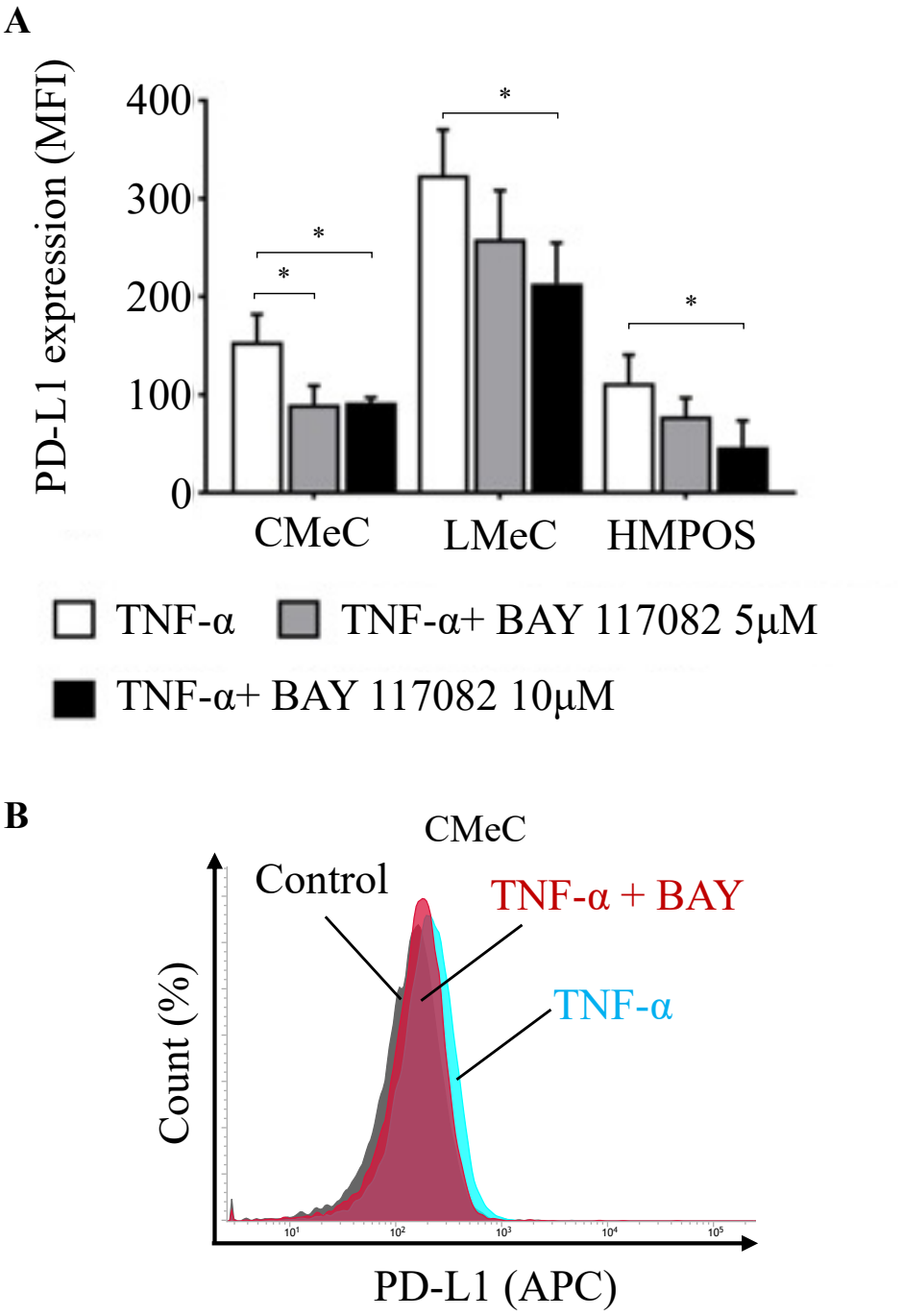

Figure I-7. Inhibition of TNF-α-induced PD-L1 expression by the NF-κB inhibitor, BAY 11-7082 in tumor cells

(A) Inhibition of TNF-α-induced PD-L1 expression due to various concentrations of BAY 11-7082. (B) Histogram analysis of PD-L1 expression on tumor cells incubated with TNF-α and BAY 11-7082. ANOVA with a post-hoc Tukey's multiple comparison test was used for statistical analysis. *$p < 0.05$.

DISCUSSION

Immune checkpoint inhibitors with promising clinical efficacy against several different tumors have been developed for use in dogs, but the ORR of ICIs is still low. In human medicine, several resistance mechanisms on the application of ICIs have been proposed, and various ICI-based combination therapies have been tested to overcome the resistance to ICIs [Jenkins *et al*., 2018]. Whereas, in dogs, resistance mechanisms to ICIs remain to be elucidated, and alternative or combination strategies are needed to improve the clinical efficacy of ICIs. It is necessary to elucidate the regulatory mechanisms of PD-L1 expression to gain insights that could help develop novel therapeutic targets or improve ICI treatment outcomes in dogs.

In TME, IFN-γ would be mostly produced by activated T cells and natural killer cells [Jorgovanovic *et al*., 2020], and IFN-γ treatment reportedly upregulated PD-L1 expression on various tumor cell lines in humans and dogs [Kondo *et al*., 2010; Maekawa *et al*., 2014]. Consistent with these observations, IFN-γ treatment markedly upregulated PD-L1 expression in the present study. TNF-α used alone also upregulated PD-L1 expression in the current study. TNF-α is mainly produced by macrophages in TME [Laha *et al*., 2021]. Previous studies reported that TNF-α treatment upregulated PD-L1 expression on tumor cell lines of humans and mice [Lim *et al*., 2016; Wang *et al*., 2017], but the relationship between TNF-α and PD-L1 expression was previously unclear in canine tumors. These results have suggested that TNF-α-mediated upregulation of PD-L1 expression is context-dependent and possibly influenced by tumor cell type, genetic or epigenetic alterations, and/or other stimulations in TME. In contrast, significant differences in PD-L1 expression were not observed in cells exposed to X-irradiation on canine tumor cell lines, whereas PD-L1 upregulation was previously demonstrated on several cancer cell lines of humans [Sato *et al*., 2017]. It was suggested that Inflammatory signaling plays a more important role in PD-L1 upregulation in TME of canine tumors following irradiation compared to DNA damage signaling.

A combination of IFN-γ and TNF-α treatment further enhanced PD-L1 expression compared with the effects on expression of IFN-γ or TNF-α alone. In previous studies, a combination treatment of TNF-α and IL-4 synergistically upregulated PD-L1 expression on human renal cell carcinoma cell lines [Quandt *et al*., 2014], whereas a

combination of TNF-α and IFN-γ treatment synergistically upregulated PD-L1 expression on human myelodysplastic syndrome blast cell lines, although PD-L1 expression was not increased by TNF-α alone [Kondo *et al*., 2010]. Because the stabilization of PD-L1 protein by CSN5 is enhanced by TNF-α through NF-κB signaling [Lim *et al*., 2016], IFN-γ-induced upregulation of *PD-L1* mRNA expression might result in higher PD-L1 protein expression under TNF-α stimulation. Determining the precise interaction between these two stimulations would be a target of future investigations.

The stimulation of IFN-γ was associated with activation of the JAK-STAT signaling pathway and upregulation of *PD-L1* mRNA expression. In addition, an inhibitor of JAK abrogated cell surface expression of PD-L1 in IFN-γ-treated tumor cells. It has been reported that IFN-γ treatment induced PD-L1 expression via several signaling pathways, including the JAK-STAT-IRF1 axis, the STAT1-MEK-ERK and NF-κB pathways in human tumors [Liu *et al*., 2007; Kondo *et al*., 2010; Garcia-Diaz *et al*., 2017]. these results may suggest that the transcriptional regulation by the JAK-STAT signaling pathway could be the dominant mechanism underlying the IFN-γ stimulation-mediated upregulation of PD-L1 expression in canine tumor cells. The extent to which these additional pathways contributed to IFN-γ-induced PD-L1 expression should also be examined in canine tumor cells.

Whereas, in the present study, TNF-α stimulation was associated with activation of the NF-κB signaling pathway, a clear association with *PD-L1* mRNA expression was only detected in LMeC. In contrast, an inhibitor of NF-κB suppressed cell surface PD-L1 expression in all TNF-α-treated tumor cells. The expression of PD-L1 in tumor cells was reported to be regulated by various mechanisms [Yi *et al*., 2021]. In addition, it has been reported that TNF-α induced PD-L1 expression at the transcriptional and post-translational level in human tumor cells [Antonangeli *et al*., 2020; Lim *et al*., 2016; Wang *et al*., 2017]. These results may suggest that transcriptional, post-transcriptional or post-translational regulation mediated by the NF-κB signaling pathway could be involved in TNF-α stimulation-induced upregulation of PD-L1 expression.

In this study, oclacitinib could successfully inhibit IFN-γ stimulation-induced PD-L1 expression. A preclinical study using a xenograft mouse model of human non-small-cell lung cancer found that the selective JAK2 inhibitor SAR302503 interfered with tumor growth and abrogated PD-L1 expression [Pitroda *et al*., 2018]; hence, JAK

inhibitors, including oclacitinib, might be useful as antitumor agents in dogs. However, concentrations of oclacitinib used in this study (2.5 or 5.0 μM) were higher than those required to inhibit JAK signaling in cells [Gonzales *et al*., 2014] and those that are pharmacologically achievable in dogs [Collard *et al*., 2014]. In this study, high concentrations of oclacitinib were required to inhibit JAK-STAT signaling pathway possibly because the JAK/STAT expression was significantly upregulated by exogenous IFN-γ treatment. Moreover, in this study, other signaling pathways were not investigated in IFN-γ-treated cells. Since PD-L1 may be upregulated by IFN-γ through not only the JAK-STAT signaling pathway but also other signaling pathways, off-target effects of oclacitinib may also contribute to the PD-L1 downregulation. Moreover, it is still unclear whether inhibition of PD-L1 induction by IFN-γ could be achieved with clinically available concentrations of oclacitinib. In addition, because JAK1/JAK2 loss-of-function has been associated with resistance to PD-1 blockade, possibly through impaired MHC class I expression [Zaretsky *et al*., 2016], effects of JAK inhibitors on antitumor immunity still require careful investigation.

The limitations of the present study included that the use of limited number of cell lines established from specific tumor types. Various regulatory mechanisms of PD-L1 expression have been reported in many human tumor cell lines [Dermani *et al*., 2019], and these may be cancer-type specific or cell-clone specific. In addition, in spontaneous tumors, complicated interactions between tumor cells and the TME were involved in the regulation of PD-L1 expression [Yi *et al*., 2021]. Thus, further studies using tumor specimens from clinical cases would be required to fully elucidate the regulatory mechanisms of PD-L1 in canine tumors.

In conclusion, these results suggest that PD-L1 was upregulated by IFN-γ and TNF-α stimulation in canine tumor cell lines through, at least in part, the JAK-STAT signaling pathway and NF-κB signaling pathway, respectively. Although further studies are necessary to fully elucidate the regulatory mechanism of PD-L1 expression in canine tumors, this study provided new insights into the role of inflammatory signaling in PD-L1 regulation. Improving our understanding of this regulatory mechanism would be an important step in discovering novel therapeutic targets and improving the effectiveness of PD-1/PD-L1–targeted immunotherapy in dogs.

SUMMARY

Expression of programmed death ligand 1 (PD-L1) on tumor cells provides an immune evasion mechanism by inducing suppression of cytotoxic T cells. Various regulatory mechanisms of PD-L1 expression have been described in human tumors; however, little is known in canine tumors. To investigate whether inflammatory signaling and DNA damage singaling is involved in PD-L1 regulation in canine tumors, effects of interferon (IFN)-γ and tumor necrosis factor (TNF)-α treatment and X-irradiation exposure were examined in canine malignant melanoma (CMeC and LMeC) osteosarcoma (HMPOS) cell lines. The protein level of PD-L1 expression was upregulated by IFN-γ and TNF-α stimulation, but not by X-irradiation exposure. Upon IFN-γ stimulation, all cell lines showed an increase in expression of *PD-L1*, *signal transducer and activator of transcription (STAT)1*, *STAT3* and genes regulated by STAT activation. Upregulated expression of these genes was suppressed by the addition of a Janus kinase (JAK) inhibitor, oclacitinib. In contrast, upon TNF-α stimulation, all cell lines exhibited higher gene expression of the nuclear factor κ B (NF-κB) gene *RELA* and genes regulated by NF-κB activation, whereas expression of *PD-L1* was upregulated in LMeC only. Upregulated expression of these genes was suppressed by the addition of an NF-κB inhibitor, BAY 11-7082. The upregulation of PD-L1 expression induced by IFN-γ and TNF-α treatment was reduced by oclacitinib and BAY 11-7082, respectively, indicating that PD-L1 upregulation by IFN-γ and TNF-α stimulation is regulated via the JAK-STAT and NF-κB signaling pathways, respectively. These results provide insights into the role of inflammatory signaling in PD-L1 regulation in canine tumors.

CHAPTER II

Enhancement of radio-sensitivity through inhibition of Janus kinase signaling by oclacitinib in canine tumor cell lines

INTRODUCTION

Radiation therapy is an effective treatment option for enhancing local tumor control in canine tumor patients, but its effectiveness is often limited, leading to frequent occurrences of local recurrence and distant metastasis after radiation therapy. Novel approaches are required to improve the outcome of radiation therapy in canine cancers.

The JAK and STAT families played pivotal roles in mediating essential cellular processes such as hematopoiesis, cell proliferation, differentiation, and apoptosis [Liu *et al*., 1997; Stephanou *et al*., 2000]. Following activation by JAK through the phosphorylation of a conserved tyrosine residue (Tyr 705), STAT translocated into the nucleus, where it regulated the transcription of specific target genes [Shuai *et al*., 1994]. Specificity in this signaling pathway was determined by the combinations of distinct JAK proteins (JAK1, JAK2, JAK3, and TYK2) and members of the STAT family (STAT1, STAT2, STAT3, STAT4, STAT5, and STAT6) [Krolewski *et al*., 1990; Wilks *et al*., 1991; Shuai *et al*., 1993; Hou *et al*., 1994; Zhong *et al*., 1994; X. Liu *et al*., 1995].

Oclacitinib, an orally available JAK inhibitor, is currently used as a therapeutic agent for canine pruritus associated with atopic dermatitis and allergic dermatitis [Barrett *et al*., 2019]. It has been shown to be safe for extended use in dogs aged 12 months or older [Cosgrove *et al*., 2015]. Oclacitinib preferentially inhibited JAK1 over JAK2 at recommended doses in the clinical setting, resulting in suppression of production of JAK1-dependent cytokines involved in allergy and inflammation, such as IL-2, IL-4, IL-6, and IL-13 with minimal effects on production of JAK2-dependent cytokines associated with hematopoiesis (granulocyte-macrophage colony-stimulating factor and erythropoietin) in cellular assays [Gonzales *et al*., 2014].

Among of JAK-STAT signaling pathway, STAT3 is well-known for its role in promoting tumor growth, and persistent STAT3 activation has been correlated with tumor progression and poor prognosis in various human cancers, including breast cancer, prostate carcinoma, and osteosarcoma [Mora *et al*., 2002; Banerjee and Resat, 2016]. Several studies have demonstrated persistent STAT3 activation, driven by factors such as G-protein coupled receptors, non-receptor tyrosine kinases, and IL-6 family cytokines.

Its activation contributed to inhibiting apoptosis signals and promoting cell proliferation, angiogenesis, and immune evasion in various human tumor cell lines, including melanoma, prostate carcinoma, and osteosarcoma [Mora *et al*., 2002; Wang *et al*., 2014; Kulesza *et al*., 2019]. Recent studies have also demonstrated persistent STAT3 activation in several canine tumors, including osteosarcoma and mammary carcinoma, which correlated to poor tumor prognosis [Król *et al*., 2011; Bid *et al*., 2012]. This activation has been found to contribute to tumor angiogenesis and apoptosis suppression in canine osteosarcoma cell lines [Bid *et al*., 2012; Couto *et al*., 2012]. Consequently, inhibiting STAT3 signaling is considered a promising therapeutic approach for both human and canine cancers.

Recently, some studies have shown radiation-induced phosphorylation of STAT3 through several mechanisms, such as augmentation of secreted phosphoprotein 1-JAK2 signaling, enhancement of EGFR or IL-6 expression, and induction of Src phosphorylation. These processes ultimately promoted tumor radio-resistance by enhancing invasiveness, DNA damage repair, and angiogenesis in several human cancer cells, including esophageal carcinoma, prostate cancer, and pulmonary adenocarcinoma [Singh-Gupta *et al*., 2009; Li *et al*., 2013; Wang *et al*., 2022]. In contrast, the JAK inhibitor suppressed persistent and radiation-induced STAT3 activation and enhanced radio-sensitivity in several cancer cells by inhibiting the expression of programmed death ligand 1, cell cycle progression, and enhancing apoptosis [Sun *et al*., 2011; Yan *et al*., 2013; Pitroda *et al*., 2018]. Additionally, a combination treatment of irradiation and a JAK or STAT3 inhibitor demonstrated radio-sensitizing effects in tumor xenograft mouse models [Lu *et al*., 2018; Pitroda *et al*., 2018; Zhang *et al*., 2022]. Therefore, regulating aberrant and increased STAT3 activation could potentially be an effective treatment of tumors that exhibit radio-resistance. In Chapter I, it was demonstrated that oclacitinib inhibited STAT1 and STAT3 activation, leading to suppressing IFN-γ–induced PD-L1 upregulation in canine osteosarcoma and malignant melanoma cell lines. These results suggested that oclacitinib could inhibit persistent and radiation-induced STAT3 activation in tumor cells and enhance the radio-sensitivity of tumor cells, but the impact of oclacitinib on tumor radio-sensitivity in canine tumors remains unclear.

The objective of this chapter of the study is to investigate the radio-sensitizing

effects of oclacitinib and to elucidate the underlying mechanisms both *in vitro* and *in vivo* using canine tumor cell lines. The radio-sensitizing effect of oclacitinib was evaluated using a clonogenic assay and a tumor growth assessment in a xenograft mouse model. The protein levels of STAT3 and poly (ADP-ribose) polymerase (PARP) through Western blotting were assessed, transcript levels of genes regulated by STAT3 were examined using RT-qPCR, and apoptosis and cell cycle were analyzed using flow cytometry.

MATERIALS AND METHODS

Cell line validation and culture condition

A canine osteosarcoma cell line (HMPOS), which was established in our laboratory [Barroga *et al*., 1999], and a malignant melanoma cell line (CMeC) provided by investigators at Tokyo University, Japan [Inoue *et al*., 2004], were utilized in this study. These cell lines have been employed in previous canine tumor research [Maekawa *et al*., 2014]. These cell lines were verified to be free from mycoplasma infection using PCR at the ICLAS Monitoring Center in Japan, and RNA-sequencing was performed to confirm their canine origin. In the present study, these cell lines were cultured in RPMI-1640 medium (Thermo Fisher Scientific) supplemented with 10% FBS (Sigma-Aldrich), 100 units/ml of penicillin G (Wako Pure Chemical Industries), and 100 μg/ml of streptomycin (Wako Pure Chemical Industries). The cultures were maintained in a humidified atmosphere with 5% CO_2 at 37°C.

X-ray irradiation and reagent

Cellular X-ray irradiation was administered using the XRAD iR-225 X-ray irradiator (Precision X-Ray) at a dose rate of 1.37 Gy/minute, operating at 200 kVp and 15 mA, with the application of a 1.0 mm aluminum filter at room temperature. Oclacitinib was obtained from MedchemExpress (Monmouth Junction). Under the conditions involving a combination of X-irradiation and oclacitinib, each cell line was incubated with the specified concentrations of oclacitinib for 4 hours, and then exposed to 5 Gy X-irradiation.

Western blotting

Western blotting was conducted using the following antibodies: Rabbit monoclonal STAT3 antibody (Cell signaling Technology), Rabbit monoclonal phospho-STAT3 antibody (Cell signaling Technology), Rabbit PARP antibody (Cell Signaling Technology), and Rabbit monoclonal β-actin antibody (Cell signaling Technology). Horseradish peroxidase-linked anti-rabbit IgG (Cell Signaling Technology) served as the secondary antibody. Each cell line (3.0×10^5 cells/well) was incubated with 500nM of

oclacitinib for 4 hours, and then they were exposed to 5 Gy X-irradiation. Subsequently, cells were gently washed three times with PBS and harvested at indicated time points post X-irradiation. Cell lysis was carried out using a radioimmunoprecipitation assay buffer (Sigma-Aldrich), supplemented with a protease inhibitor cocktail (Sigma-Aldrich) while maintaining samples on ice. After centrifugation at 13,000 × g at 4°C for 20 minutes, supernatants were collected. Protein concentration was measured using a Protein Quantification Assay Kit (Macherey-Nagel, Dürren, Germany). Three μg of protein from each sample was separated by 4-12% sodium dodecyl sulfate-polyacrylamide gel electrophoresis, followed by transferring onto polyvinylidene difluoride membranes. These membranes were then incubated in 3% bovine serum albumin (Sigma-Aldrich) in PBS containing 0.1% Tween 20 for 1 hour. Primary antibodies for STAT3 (1:1000), phospho-STAT3 (1:1000), PARP (1:1000), and β-actin (1:5000) were applied and incubated overnight at 4°C. Subsequently, the membranes were incubated with HRP-linked secondary antibodies (1:3000 for STAT3 and phospho-STAT3, 1:10000 for β-actin) for 1 hour, and then they were exposed to Western Blot Ultra-Sensitive HRP substrate (TAKARA Bio Inc., Kusatsu, Japan) for 5 minutes immediately before detection. Chemiluminescence was observed using an Image Quant LAS 4000(GE Healthcare, Buckinghamshire, UK). The intensity of each band was analyzed employing ImageJ software (NIH, Bethesda, MD, USA). Phospho-STAT3 and cleaved PARP values were normalized to STAT3 and PARP, respectively. The protein levels in all groups were normalized to those in the control group.

Clonogenic assay

Each cell line was plated at varying concentrations in 60-mm culture dishes. The cells were cultured for 4 hours with different concentrations of oclacitinib, followed by exposure to varying doses of X-ray irradiation. Twenty-four hours after irradiation, the culture medium was replaced with fresh medium. After 7 days of incubation, the cells were fixed using ethanol and subsequently stained with Giemsa's solution (Wako Pure Chemical Industries). Colonies consisting of more than 50 cells were counted as colony-forming units. Three independent experiments were conducted, and plating efficiency was calculated. Survival fractions were then determined, with plating efficiency of the

unirradiated control being considered for correction, and dose-response curves were generated. A linear-quadratic model was then applied to fit the survival curves, represented as SF = ($-\alpha D-\beta D^2$), with SF denoting the surviving fraction and D representing the physical dose.

RT-qPCR

Each cell line (3.0×10^5 cells/well) was exposed to 5 Gy X-irradiation followed by 4 hours of incubation with 500nM of oclacitinib, then incubated for 24 hours. Following harvesting cells, cells were subjected to total RNA extraction using TRIZol reagent (Thermo Fisher Scientific). Quantification of total RNA was then performed by spectrophotometry with the wavelength at 260 nm. Subsequently, 500 ng of RNA was subjected to reverse-transcription into cDNA using M-MLV RT kit (Thermo Fisher Scientific) in a 20 µl reaction. Duplicate qPCR analyzes were then conducted for each sample utilizing the KAPA SYBR FAST qPCR Master Mix (2×) Kit (KAPA Biosystems, Wilmington, MA, USA). For each sample, a total volume of 20 µl was prepared, consisting of 10 µl of KAPA master mix, 200nM specific primers, and 1 µl cDNA. No template controls were included by adding nuclease-free water. The qPCR conditions comprised an initial denaturation at 95°C for 2 minutes, followed by 40 cycles of denaturation at 95°C for 15 seconds, annealing at 60°C for 20 seconds, and extension at 72°C for 1 minute. Relative mRNA expressions were calculated using the reference gene, *GAPDH*, and quantification was performed using the delta–delta Ct method [De Bruin *et al*., 2005]. The primer sequences used in the experiments [Sano *et al*., 2005; Couto *et al*., 2012; Bwalya *et al*., 2017; Akaraphutiporn *et al*., 2020; Wang *et al*., 2023] are provided in Table II-1. All primers were previously utilized in canine tumor studies. The primers were designed to detect all transcript variants. While the primers for *GAPDH*, *Survivin*, *CCND1*, and *myeloid cell leukemia 1* (*MCL1*) involved spanning exon-exon junctions, the other primers could not span the junction due to the absence of exon structure information in the National Centre for Biotechnology Information database (https://www.ncbi.nlm.nih.gov/). The qPCR efficiency of these primers ranged from 97 to 102%. The specificity of the primer pairs was confirmed through a single melting peak

in the melting curve analysis. Additional details regarding the primers used in this study are available in Table II-2.

Apoptosis analysis

Each cell line (3.0×10^5 cells/well) was incubated with 500nM of oclacitinib for 4 hours before exposure to 5 Gy X-irradiation. Cells were incubated for 24 hours after X-irradiation, then harvested and subjected to double staining with annexin V and propidium iodide using the Annexin V Apoptosis Detection Kit I (BD Biosciences) according to the manufacturer's protocol. The apoptosis rate of cells was assessed using a BD FACS Verse Flow Cytometer (BD Biosciences).

Cell cycle analysis

Each cell line (3.0×10^5 cells/well) was exposed to 5 Gy X-irradiation followed by 4 hours of incubation with 500nM of oclacitinib, then incubated for 24 to 48 hours. Then, cells were harvested in 1.5 mL polypropylene tubes and subsequently stained with Cell Cycle Assay Solution Deep Red (Dojindo, Kumamoto, Japan), following the manufacturer's instructions. The cells were then examined and categorized in to G1, S, and G2 phase based on their DNA content using a BD FACS Verse Flow Cytometer (BD Biosciences).

Xenograft tumor volume assessment

To assess the impact of oclacitinib on *in vivo* tumor growth, the tumor growth was evaluated using a tumor xenograft mouse model. A mixture of 1.0×10^5 cells of HMPOS in 50 µl of PBS and 50 µl of Matrigel (BD Biosciences) were injected subcutaneously into the left hind legs of 7-week-old female BALB/cAJcl-nu/nu mice (CLEA Japan, Inc., Tokyo, Japan). The tumor volumes [Volume = length × $(\text{width})^2/2$] and body weight were measured daily. When tumors reached 100 mm^3, the mice were randomly divided into four groups: (A) control, (B) oclacitinib, (C) X-irradiation, and (D) X-irradiation and oclacitinib. The Number of mice used in each group was seven. For group (B) and (D), oclacitinib dissolved in 0.1 ml of saline was administered orally at doses of 10 mg/kg twice a day for 10 days, whereas for group (A) and (C), the same

volume of saline was provided as vehicle control twice a day. The mice in group (C) and (D) were anesthetized by isoflurane inhalation with oxygen, the body was covered with a 2-mm-thick lead sheet, and tumor-bearing legs were locally exposed to 20 Gy X-irradiation in a single dose 3 days after starting administration of oclacitinib or saline. At the end of the assessment period, mice were humanely sacrificed using inhalation of CO_2 gas. All animal experiments were performed according to Hokkaido University Institutional Animal Care and Use Committee guidelines (approval number: 23-0122).

Statistical analysis

All results in this study are shown as mean ± SD. Statistical analysis was carried out utilizing GraphPad Prism 9 software (GraphPad Software, San Diego, CA, USA). The normality of the data distribution was assessed using the Shapiro-Wilk test. For the comparison of two groups, the Mann-Whitney *U* test was used in case the values were not normally distributed or if the sample size was small, whereas an unpaired, two-tailed Student's *t*-test was performed when the data followed a normal distribution. For cases involving three or more groups, ANOVA followed by Tukey's multiple comparison test was conducted for data analysis. The Kaplan-Meier method was used for generating survival curves and the statistical analysis was performed using the log-rank test for the xenograft tumor volume measurement. A p-value < 0.05 was considered statistically significant.

Table II-1 Primer pairs used for RT-PCR

Gene	Forward primer 5'-3'	Reverse primer 5'-3'
BCL-x_L (BCL2L1)	GGCCTTTTTCTCCTTCGGTG	CTCTCGGCTGCTGCATTGTT
CCND1	AGTGTGATGCGGACTGTCTC	GCGCACCCTCAAATGTTCAC
CDK4	TAGCTTGCGGCCTGTCTATG	CAGAGAAGACCCTCACTCGG
CDK6	AGCCAAACGTCCCTAGAAGC	GAGAGATGCCTGGTAGACGC
GAPDH	CTGAACGGGAAGCTCACTGG	CGATGCCTGCTTCACTACCT
MCL1	CAACCACGAGACAGCCTTCCAAG	CACTGAAAACATGGACAATCAC
Survivin (BIRC5)	GAAGGCTGGGAGCCAGATGATG	CGCACTTTCTTTGCGGTCTC

Table II-2 Primer details for RT-PCR

Gene (Official gene symbol)	Amplicon length (bp)	Target exons	Linear dynamic range (copies)	qPCR efficiency (%)
BCL-x_L (BCL2L1)	186	-	10^3–10^8	100
CCND1	184	4-5	10^3–10^8	101
CDK4	145	-	10^4–10^8	97
CDK6	121	-	10^3–10^5	102
GAPDH	129	8-10	10^3–10^5	100
MCL1	101	2-3	10^4–10^8	98
Survivin (BIRC5)	203	2-4	10^3–10^5	99

RESULTS

Induction of STAT3 activation in X-irradiated cells in a dose- and time-dependent manner

Western blotting was performed to assess the alterations of STAT3 expression and STAT3 phosphorylation by X-irradiation. At 24 hours after exposure to 5 Gy X-irradiation, STAT3 activation was significantly induced and dose-dependently upregulated in HMPOS. Whereas STAT3 activation was similarly increased until 5 Gy X-irradiation, there was not much change observed in 5-10 Gy X-irradiation in CMeC (Figure II-1A and B). In cells exposed to 5 Gy X-irradiation, its expression was significantly enhanced in a time-dependent manner in both tumor cell lines (Figure II-1C and D).

The radio-sensitizing effect of oclacitinib in vitro and its ability to inhibit STAT3 activation

To investigate the radio-sensitizing effect of oclacitinib, a clonogenic assay was conducted. Firstly, to test the cytotoxicity of oclacitinib itself, cells were treated with various concentrations of oclacitinib for 24hours. Cell viability was decreased after exposure to oclacitinib in both tumor cell lines (Figure II-2A). Therefore, 500nM was chosen as the optimal concentration of oclacitinib for subsequent experiments to keep the cell viability at acceptable levels (> 60%) while maintaining the effective dosage to exert the inhibitor activity in the cell culture. Next, the survival of colonies was quantified after X-irradiation with 500nM of oclacitinib in the tumor cell lines. Oclacitinib significantly enhanced cell death induced by X-irradiation and decreased colony formation compared to the control (without oclacitinib) in both tumor cell lines (Figure II-2B). In addition, Western blotting was performed to confirm the inhibitory effect of STAT3 activation following treatment with oclacitinib. Oclacitinib significantly suppressed X-irradiation-induced STAT3 activation in both tumor cell lines (Figure II-3A and B).

Induction of apoptosis after treatment with a combination of X-irradiation and oclacitinib

According to Western blotting analysis, PARP activation was significantly induced in cells treated with X-irradiation. The combination of X-irradiation and oclacitinib treatment further enhanced PARP activation compared to the effect of X-irradiation alone in HMPOS, but not in CMeC (Figure II-3A and C). To evaluate anti-apoptotic genes, the mRNA expression of *Survivin*, *B-cell lymphoma-extra large* (*Bcl-x_L*), and *MCL1* were analyzed using RT-qPCR. *Bcl-x_L* and *MCL1* expressions, but not *survivin* expression, were significantly suppressed in HMPOS treated with oclacitinib compared to cells without any treatments. In addition, all the gene expressions significantly decreased in cells treated with the combination of X-irradiation and oclacitinib compared to cells treated by X-irradiation alone. Although the same trend was observed by each treatment, differences in the gene expressions did not re ach statistical significance in CMeC (Figure II-4A). Next, cells stained with annexin V were designated as those undergoing apoptosis, and cell apoptosis rate was examined in cells treated with X-irradiation and oclacitinib using annexin V staining. The proportion of apoptotic cells was significantly increased in cells treated with X-irradiation alone and the combination of both treatments in both tumor cell lines. The apoptotic cell proportion was further increased in cells treated with the combination of both treatments compared to cells treated with either oclacitinib or X-irradiation alone in HMPOS, but not in CMeC (Figure II-5). The apoptotic cell rates in HMPOS and CMeC cells were as follows: 8.11 ± 0.6% and 4.95 ± 0.11% under control conditions; 18.07 ± 0.59% and 3.15 ± 0.05% following oclacitinib treatment; 18.11 ± 0.69% and 8.38 ± 0.11% following X-irradiation; 27.53 ± 0.38% and 7.01 ± 0.46% following X-irradiation and oclacitinib treatment, respectively.

Inhibition of cell cycle progression from G1 to later phases by oclacitinib treatment

To evaluate cell cycle regulating genes, the mRNA expression of *CCND1*, *cyclin-dependent kinase (CDK) 4* and *6* were analyzed using RT-qPCR. All the gene expressions in HMPOS and all the gene expressions except for *CCND1* in CMeC were significantly inhibited in cells treated with oclacitinib and the combination of X-irradiation and oclacitinib compared to cells without any treatments and cells treated with X-irradiation alone, respectively. Furthermore, X-irradiation significantly upregulated *CCND1* and *CDK6* gene expression compared to no treatment control in HMPOS (Figure II-4B). Next, to assess the proliferative activity of each tumor cell line with exposure to X-irradiation

and oclacitinib, cell cycle analysis was conducted using flow cytometry. After 24 hours of X-irradiation, a significant increase in the G1 ratio and a significant decrease in the G2 ratio was observed in cells treated with oclacitinib alone compared to no treatment control, as well as in cells treated with the combination of X-irradiation and oclacitinib compared to X-irradiation alone in both tumor cell lines. After 48 hours of X-irradiation, a similar trend was observed in cells treated with the combination of X-irradiation and oclacitinib compared to X-irradiation alone in both tumor cell lines. (Figure II-6).

Enhancement of tumor growth delay following treatment of a combination of X-irradiation and oclacitinib

In further investigation of the radio-sensitizing effects of oclacitinib *in vivo*, HMPOS cells were injected subcutaneously into immunodeficient nude mice, and tumor growth was assessed. The tumor volume of mice treated with X-irradiation was dramatically reduced, whereas oclacitinib treatment alone did not decrease the tumor volume compared to mice without any treatment (control). Tumor growth in mice treated with a combination of X-irradiation and oclacitinib was significantly delayed compared to mice treated with X-irradiation alone (Figure II-7A). The time needed for a 2-fold increase in tumor volume in mice treated with X-irradiation alone was 18 days (with a range of 15 to 26 days), while for mice treated with X-irradiation and oclacitinib, it was 29 days (with a range of 23 to 60 days) after assignment (Figure II-7B). The time required for a 2-fold increase in tumor volume between mice treated with X-irradiation and oclacitinib was significantly longer than those treated with X-irradiation alone. In two mice treated with a combination of X-irradiation and oclacitinib, the tumor volume did not increase even after 60 days from assignment.

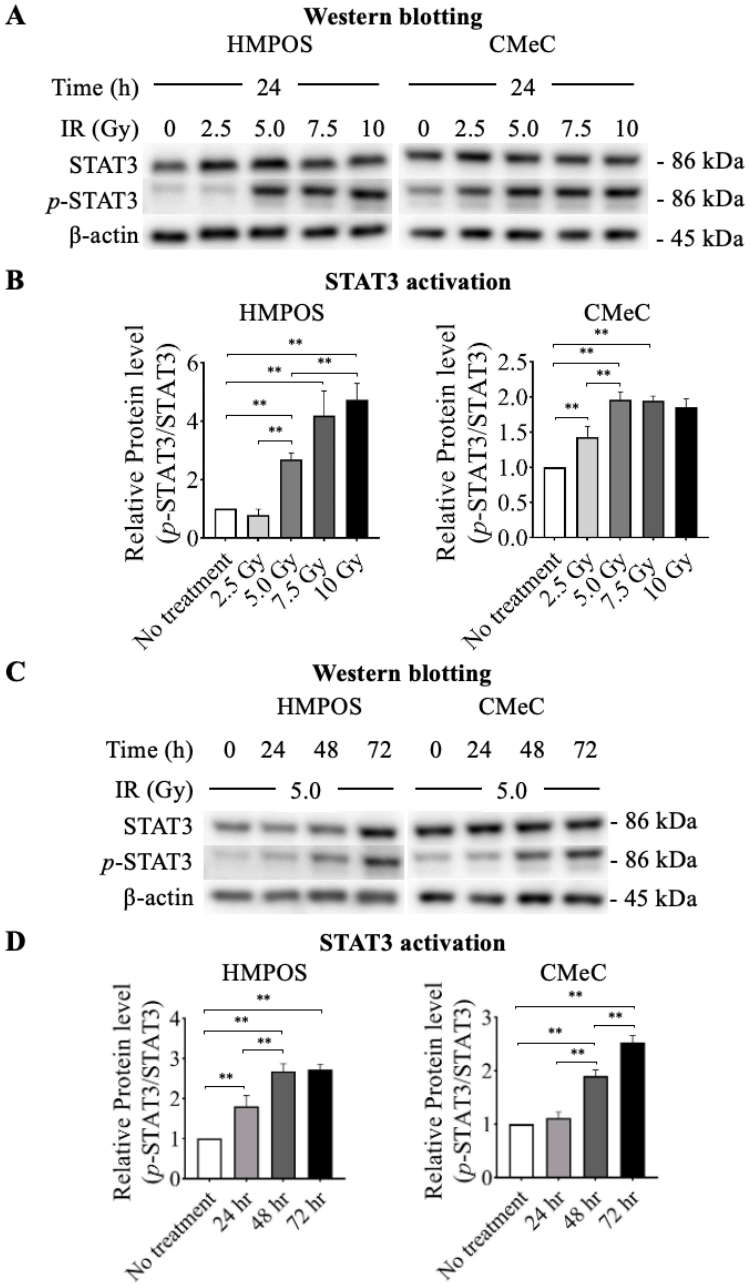

Figure II-1. Induction of STAT3 protein activation in canine tumor cells exposed to X-irradiation, depending on dose and time

(A) Analysis of STAT3 and phosphorylated STAT3 (*p*-STAT3) in cells 24 hours after 2.5-10 Gy X-irradiation (IR). (B) Comparison of the expression level of p-STAT3 relative to the corresponding total proteins. (C) Analysis of STAT3 and *p*-STAT3 expression in cells 24-72 hours following treatment with IR. (D) Comparison of the expression level of *p*-STAT3 relative to the corresponding total proteins. Statistical significance was analyzed by Tukey's multiple comparison test. $^{**}p < 0.01$.

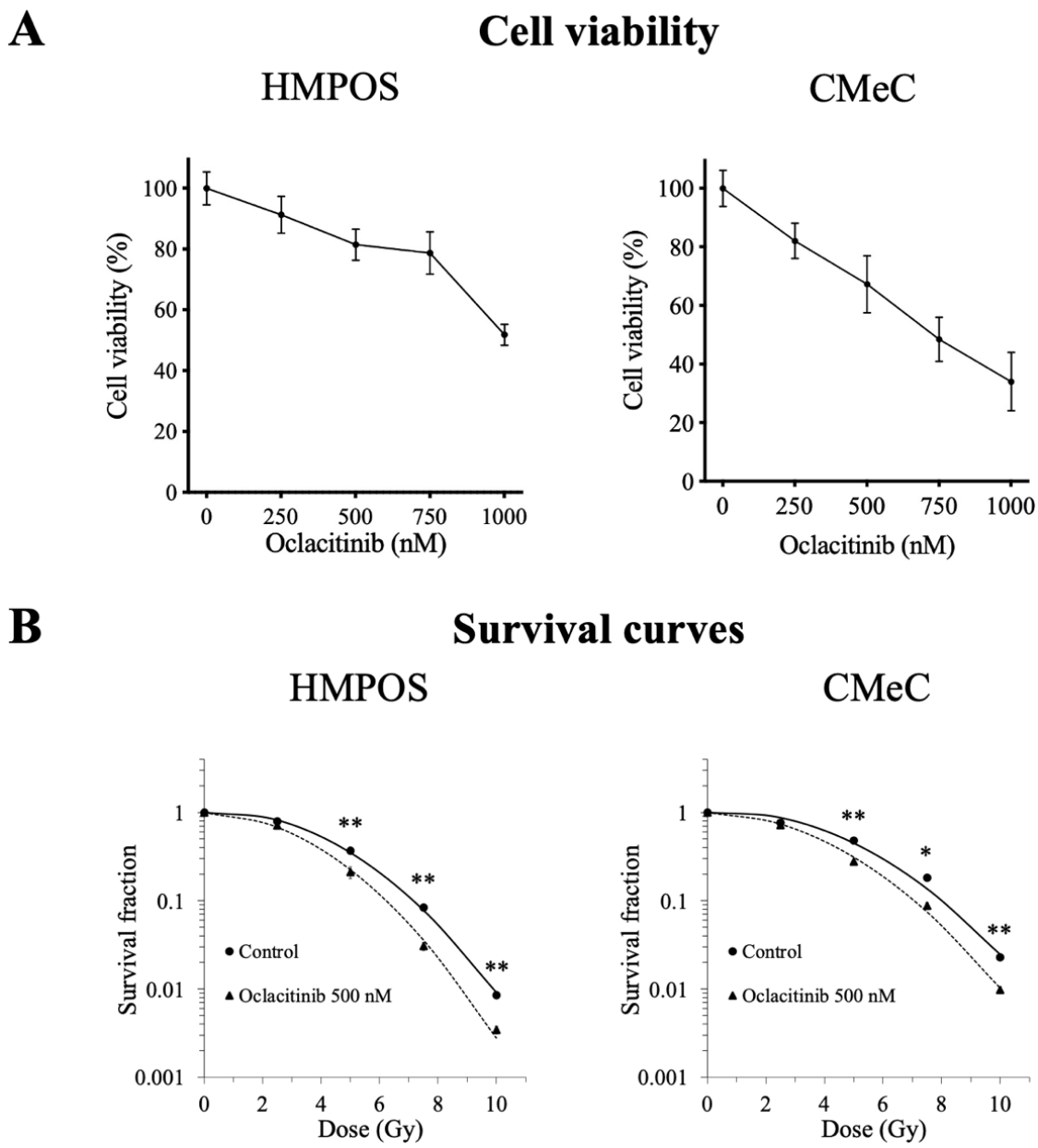

Figure II-2. Radio-sensitizing effects by oclacitinib in canine tumor cell lines

(A) Cell viability following treatment with 250-1000nM of oclacitinib. (B) Survival curves of cell colonies after X-irradiation in cell cultures treated with or without 500nM of oclacitinib. The error bars represent the SD of the mean calculated from three separate and independent experiments. Student's *t*-test was used to compare the two groups. *$p <$ 0.05 and **$p < 0.01$.

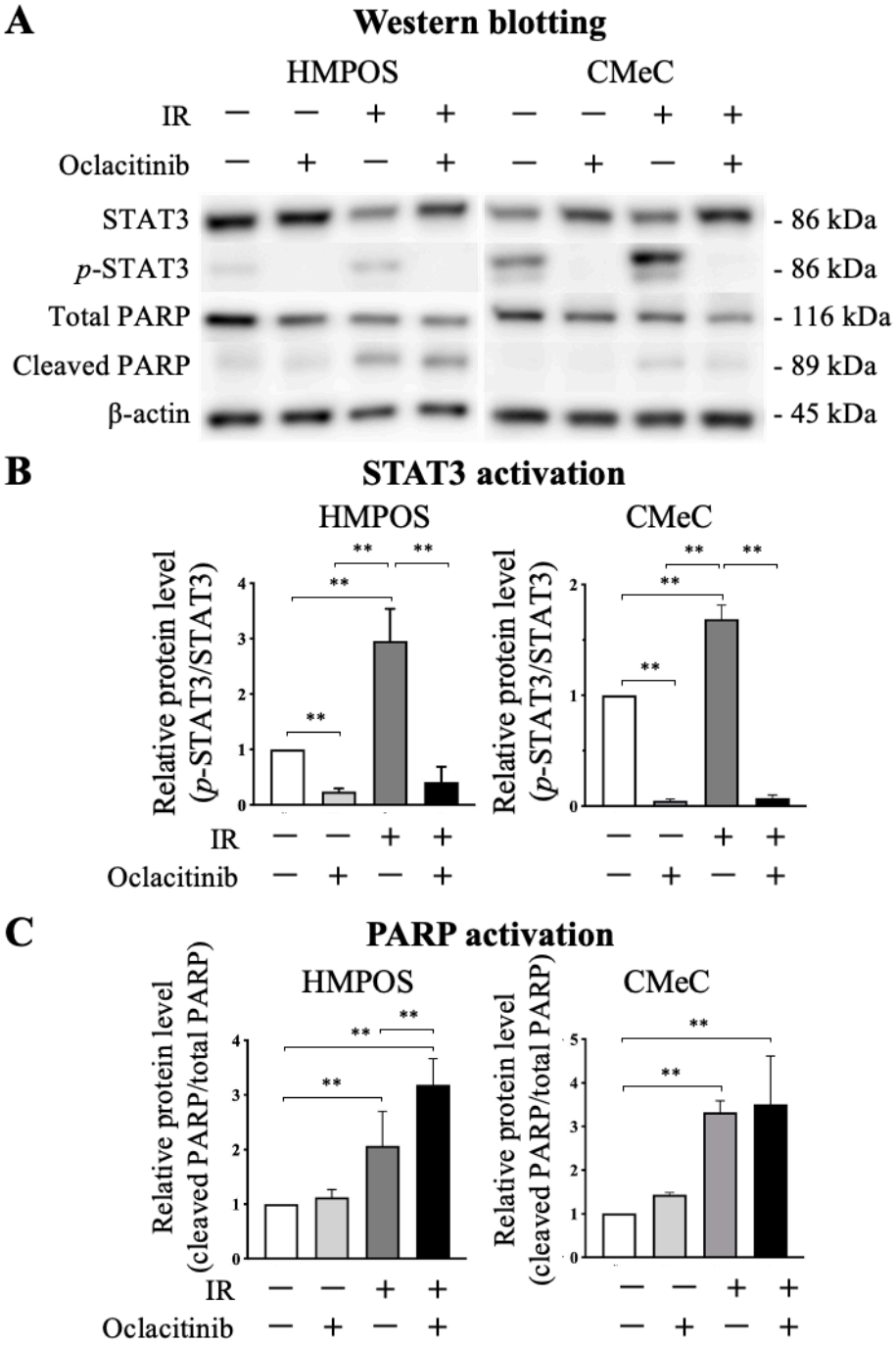

Figure II-3. Effects of X-irradiation and oclacitinib on STAT3 and PARP activation in canine tumor cell lines

(A) Analysis of STAT3, phosphorylated STAT (*p*-STAT3), total PARP, and cleaved PARP expression in cells 24 hours after 5 Gy X-irradiation (IR) with or without 500 nM of oclacitinib. (B) Comparison of the expression level of *p*-STAT3 and cleaved PARP relative to the corresponding total proteins. Statistical significance was analyzed by Tukey's multiple comparison test. $^{**}p < 0.01$.

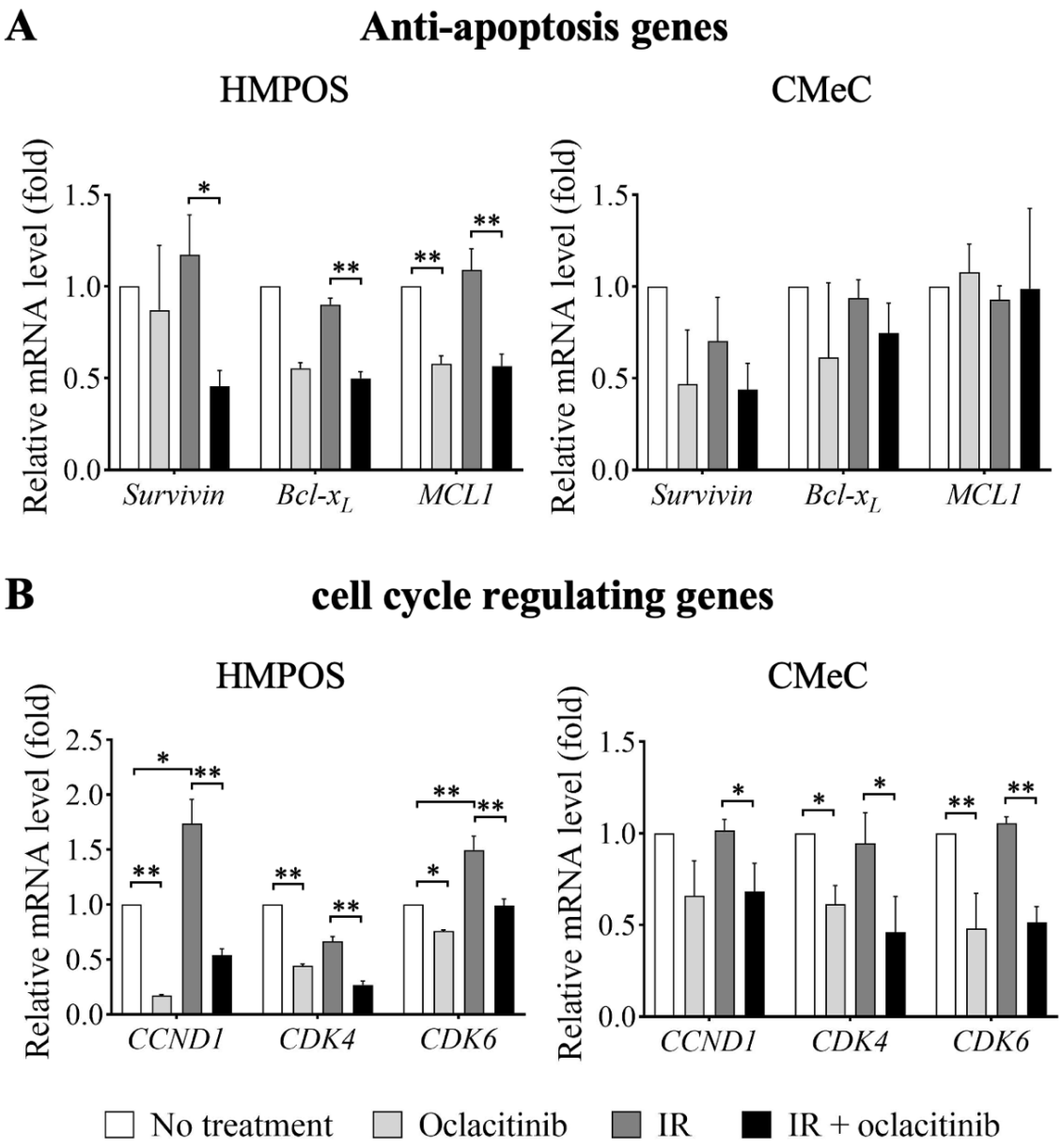

Figure II-4. Gene expression in canine tumor cell lines after X-irradiation (IR) treatment with or without oclacitinib

(A) Relative mRNA levels of *survivin*, *Bcl-x*$_L$, and *MCL1* quantified using RT-qPCR in each condition. (B) Relative mRNA expression levels of *CCND1* and *CDK4/6* quantified using RT-qPCR in each condition. Statistical significance was analyzed by Tukey's multiple comparison test. *$p < 0.05$ and **$p < 0.01$.

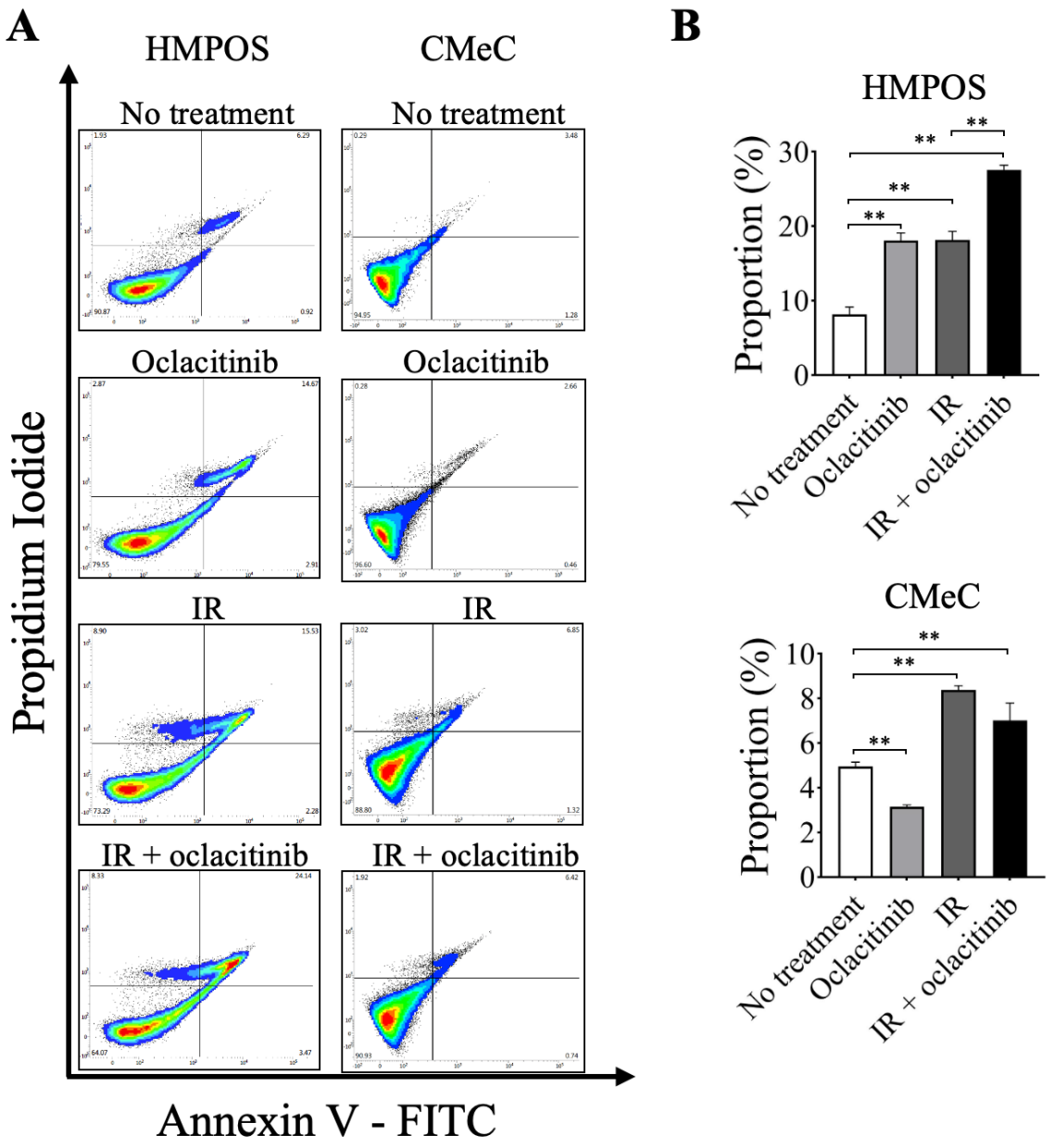

Figure II-5. Effect of X-irradiation and oclacitinib on apoptosis induction in canine tumor cell lines

(A) Analysis of apoptosis in cells after exposure to 5 Gy X-irradiation (IR) with or without 500nM of oclacitinib using flow cytometry with propidium iodide and annexin V. (B) Effects of IR and 500nM of oclacitinib on the proportion of apoptotic cells. Statistical significance was analyzed by Tukey's multiple comparison test. *$p < 0.05$ and **$p < 0.01$.

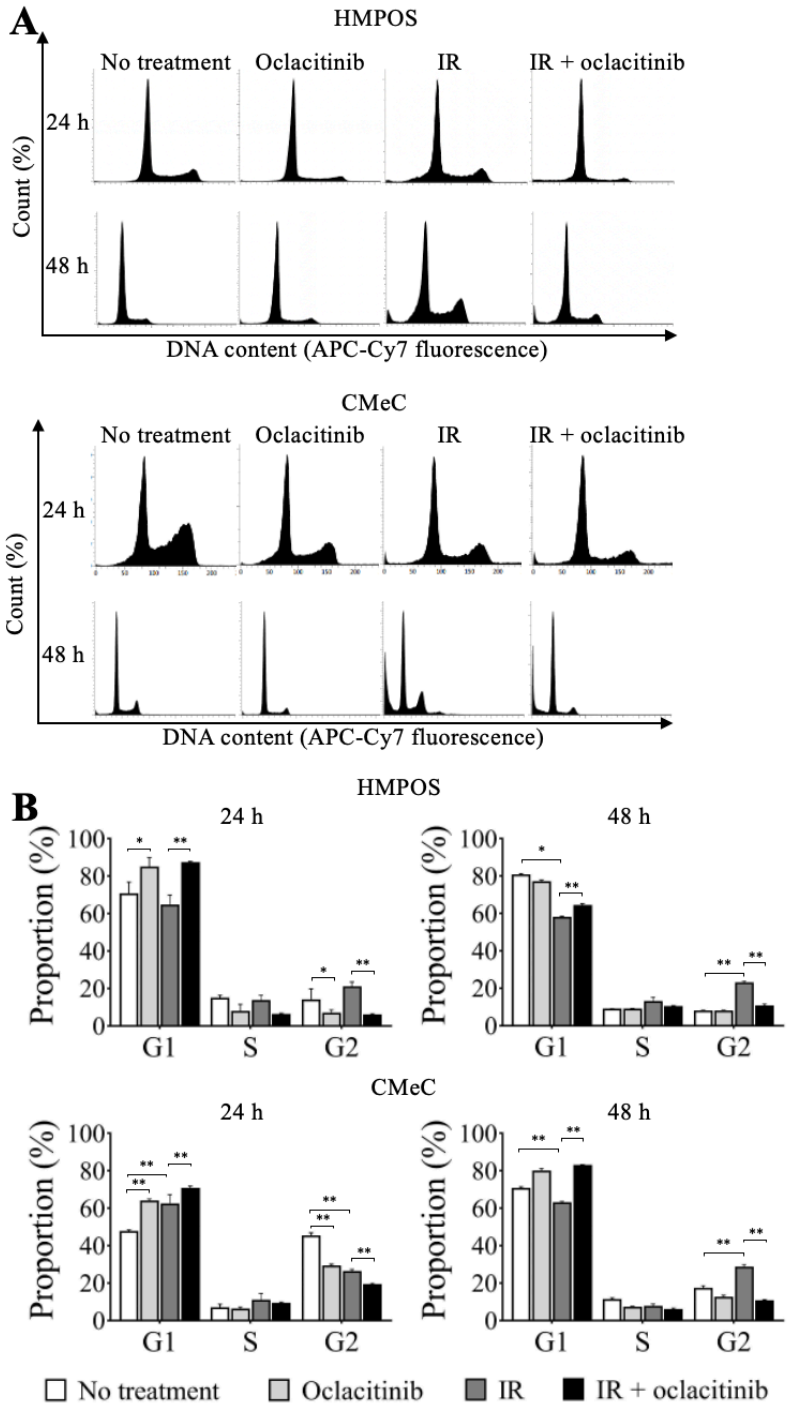

Figure II-6. Inhibition of the cell cycle progression from the G1 phase to subsequent phases in canine tumor cell lines due to oclacitinib treatment

(A) Analysis of DNA contents in cells treated with X-irradiation (IR) and oclacitinib using flow cytometry. (B) The cell distribution in different cell cycle phases 24 and 48 hours after IR treatment with or without oclacitinib. Statistical significance was analyzed by Tukey's multiple comparison test. *$p < 0.05$ and **$p < 0.01$.

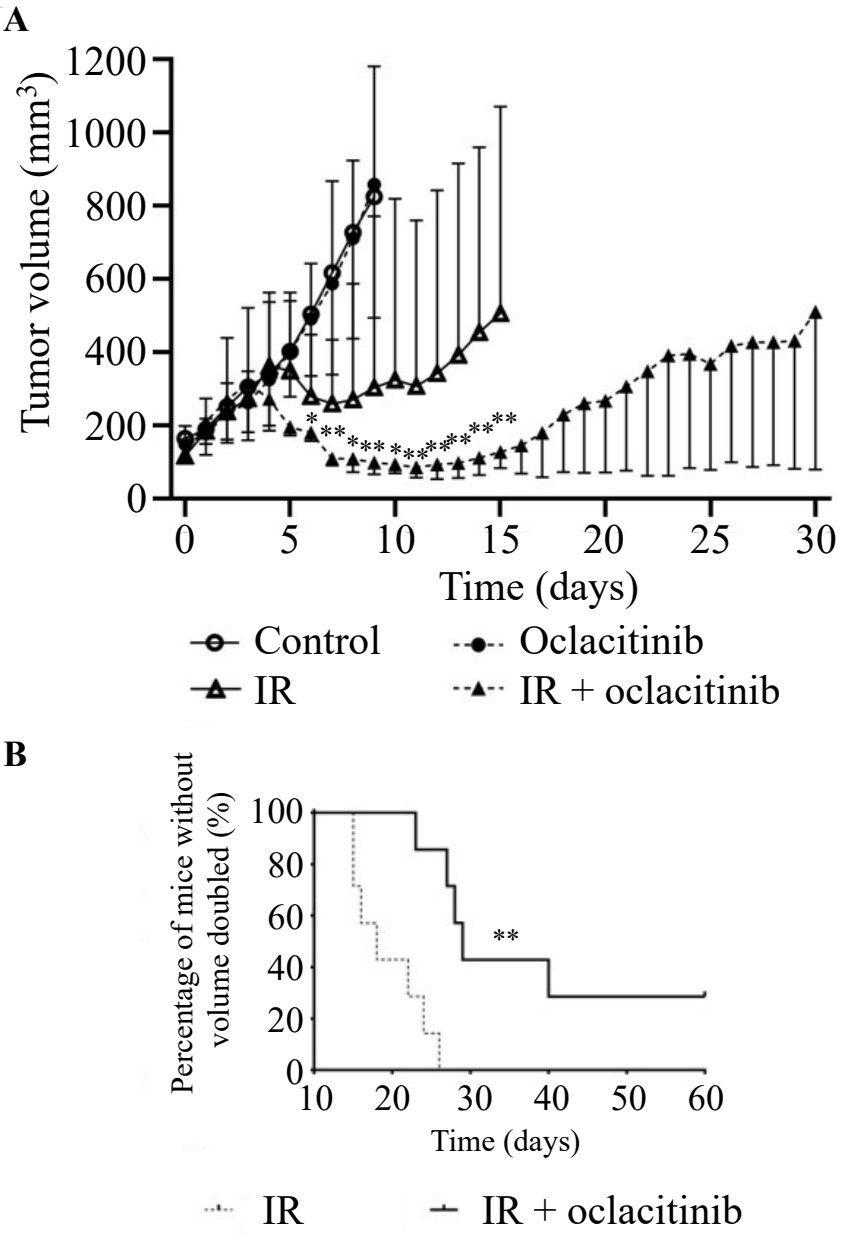

Figure II-7. Tumor growth delay due to a combination of X-irradiation and oclacitinib in xenograft mice

(A) Changes in tumor volume after assigning in each group as follows; control, oclacitinib, X-irradiation (IR), and IR + oclacitinib. (B) The Kaplan-Meier curves for the percentage of mice without volume doubled after IR. The error bars represent the range of the tumor volume for each condition. The Mann-Whitney *U* test was used to compare the change in xenograft tumor volume of IR and IR + oclacitinib. The log-rank test was used to compare the percentage of mice without volume doubled after IR. $*p < 0.05$ and $**p < 0.01$.

DISCUSSION

Oclacitinib is known to be an orally available JAK inhibitor as a therapeutic agent for canine allergic dermatitis. In human medicine, some reports have shown that inhibition of the JAK-STAT3 signaling pathway was associated with anti-cancer effects *in vitro* and *in vivo* through various mechanisms, including suppression of anti-apoptosis signals and establishment of immune evasion [Sun *et al*., 2011; Pitroda *et al*., 2018; Zhang *et al*., 2022]. Whereas a combination therapy of chemotherapy and oclacitinib in tumor-bearing dogs has already been reported, the study aimed to assess the safety and toxicity of the combination therapy [Barrett *et al*., 2019]. Therefore, the anticancer effects of oclacitinib are still unclear. The present study demonstrates the potential radio-sensitizing effects of oclacitinib on canine tumor cells through inhibition of STAT3 activation thereby promoting cell apoptosis and cell cycle arrest.

It has been reported that STAT3 activation was upregulated in cells after exposure to X-irradiation in several human tumor cell lines [Lau *et al*., 2015; Wang *et al*., 2021], but it was previously unclear whether this is also the case in canine tumors. Consistent with previous observations in human tumors, X-irradiation promoted the dose- and time-dependent induction of STAT3 activation in canine tumor cell lines. Previous studies have shown that persistent and increased induction of STAT3 activation promoted tumor migration, invasion, DNA repair, and angiogenesis, leading to tumorigenesis and tumor radio-resistance in human studies [Gao *et al*., 2014; Lau *et al*., 2015; Wang *et al*., 2021]. Therefore, it has been suggested that irradiation-induced STAT3 activation may contribute to tumor radio-resistance in canine tumors.

Clonogenic assay was performed in various concentrations of oclacitinib alone to determine the optimal concentration of oclacitinib for clonogenic assay with X-irradiation. The radio-sensitivity of both tumor cell lines was significantly facilitated by 500nM of oclacitinib. In addition, 500nM of oclacitinib dramatically inhibited X-irradiation–induced STAT3 activation in both tumor cell lines. It has been reported that STAT3 activation in tumor cells after exposure to X-irradiation was promoted through various mechanisms, including the secreted phosphoprotein 1-JAK2-STAT3 axis, IL-6 or EGFR signaling, and Src-STAT3 axis in human tumor cell lines [Singh-Gupta *et al*., 2009; Gao *et al*., 2014; Wang *et al*., 2022]. These results suggest that oclacitinib could exhibit

radio-sensitizing effects on tumor cells by inhibiting the JAK-STAT3 signaling pathway, and the JAK-STAT3 signaling pathway could be the dominant mechanism underlying X-irradiation-induced STAT3 activation in canine tumor cells.

Inhibition of STAT3 signaling by oclacitinib was associated with enhanced activation of PARP, a marker of apoptosis. Additionally, the mRNA expression of anti-apoptotic genes was significantly suppressed by oclacitinib in HMPOS, but not in CMeC. Consequently, apoptosis in cells treated with a combination of these treatments was significantly promoted compared to those following treatment with X-irradiation alone in HMPOS. Survivin is one of the most important anti-apoptotic proteins and is highly expressed in several human cancers and canine osteosarcoma [Lu *et al*., 2004; Iwasa *et al*., 2008; Fossey *et al*., 2009]. Several studies have shown that inhibition of survivin expression enhanced apoptosis, leading to enhancement of tumor radio-sensitivity [Lu *et al*., 2004; Iwasa *et al*., 2008]. Another study showed that STAT3 activation suppressed apoptosis through activation of the BCL-2 family proteins, including BCL-2, BCL-$x_{L,}$ and MCL1 by regulating the expression of the heat shock protein 70 and inhibiting c-Jun N-terminal kinase pathway [Zorzi and Bonvini, 2011]. These findings may indicate that inhibition of STAT3 signaling by oclacitinib could induce apoptosis and enhance radio-sensitivity by suppressing the anti-apoptotic mechanisms in canine tumor cells, although this effect may vary depending on the tumor cell type.

The results of our study showed that the gene expressions of *CCND1* and *CDK4/6* were significantly suppressed by the treatment with oclacitinib. Cell cycle progression leads to cell proliferation and is regulated by various cyclins and their CDK-binding partners [Bertoli *et al*., 2013]. It has been reported that cyclin D1 and CDK4/6 adjust the progression of the G1 phase and cyclin D1 was regulated by STAT3 signaling [Hydbring, *et al*., 2016; Pan *et al*., 2021]. Previous studies also reported cyclin D1 promoted tumor progression and tumor radio-resistance [Im *et al*., 2023]. In cell cycle analysis, X-irradiation significantly promoted the cell cycle progression in 48 hours post-X-irradiation in all tumor cell lines. Oclacitinib suppressed the cell cycle progression from the G1 phase to subsequent phases at both 24 and 48 hours after X-irradiation in both tumor cell lines. These results suggest that oclacitinib demonstrated a radio-sensitizing effect by inhibiting the cell cycle progression from the G1 phase to subsequent phases through inhibition of cyclin D1 expression. In contrast, cells 24 hours after

treatment with X-irradiation significantly inhibited its progression compared to cells without any treatments in CMeC. Previous studies reported that cells showed a transient delay in the G1 phase of the cell cycle after radiation exposure to repair critical DNA damage, with this delay being dose-dependent [Licursi *et al*., 2020]. In the experimental protocol, 5 Gy X-irradiation was administered to cells, and this might have led to a transient delay in the G1 phase 24 hours after treatment with X-irradiation in CMeC.

Our results showed that a combination of X-irradiation and oclacitinib significantly extended tumor regrowth delay compared to X-irradiation alone in mice transplanted with HMPOS, suggesting the potential of oclacitinib as a radiosensitizer in canine tumors. Although any adverse effects were not observed in mice following treatment with oclacitinib and a combination of X-irradiation and oclacitinib, and higher concentrations of oclacitinib (45 mg/kg) were previously used in mice study [Fukuyama *et al*., 2015], concentrations of oclacitinib administered in this study (10 mg/kg BID) were still higher than those that are clinically available in dogs [Collard *et al*., 2014]. Chapter I demonstrated that oclacitinib inhibited PD-L1 expression induced by IFN-γ on canine tumor cell lines through suppression of the JAK-STAT signaling pathway. In this study, immunodeficient mice were employed due to the use of canine tumor cell lines. Therefore, the impact of oclacitinib on the immune response to radiation exposure in a normal TME, including PD-L1 expression, could not be observed. Further analysis is required to determine whether oclacitinib might demonstrate a radio-sensitizing potential within a normal TME and to investigate its radio-sensitizing effects in clinical applications.

In summary, oclacitinib demonstrated radio-sensitizing effects on canine tumor cells in both *in vitro* and *in vivo* settings by enhancing apoptosis and inhibiting cell cycle progression. These results imply the clinical therapeutic potential of oclacitinib in combination with radiotherapy to improve treatment effectiveness and outcomes in dogs.

SUMMARY

The Janus kinase (JAK) and signal transducer and activator of transcription (STAT) signaling pathways are essential for cellular processes. Among these, STAT3 activation contributes to radio-resistance in various tumors of human and dogs. Oclacitinib, an orally administered JAK inhibitor, has gained approval for treating atopic dermatitis in dogs. However, the antitumor effects of oclacitinib are still unclear. This study aimed to investigate the radio-sensitizing effect of oclacitinib in canine tumors and to probe the underlying mechanisms using osteosarcoma (HMPOS) and malignant melanoma (CMeC) cell lines. Oclacitinib significantly enhanced the radio-sensitivity of tumor cells both *in vitro* and *in vivo*. In cells exposed to X-irradiation, STAT3 was significantly activated in a dose- and time-dependent manner, which was effectively suppressed by oclacitinib. Oclacitinib significantly enhanced radiation-induced apoptosis by inhibiting the expression of anti-apoptosis genes (*survivin, B cell lymphoma-extra large,* and *myeloid cell leukemia 1*) and Poly (ADP-ribose) polymerase protein in HMPOS only. Additionally, oclacitinib significantly inhibited the transcription of cell-cycle regulating genes (*CCND1, CDK4 and 6*) and arrested cell cycle progression from the G1 phase to subsequent phases. In conclusion, oclacitinib enhanced radio-sensitivity both *in vitro* and *in vivo* by triggering apoptosis and impeding cell cycle progression via STAT3 inhibition in canine tumor cell lines. This study suggested the clinical therapeutic potential of oclacitinib in combination with radiation therapy, aiming to enhance treatment efficacy and outcomes in dogs with tumors.

CONCLUSION

Radiation therapy is an effective treatment modality for tumors in both humans and animals. In many patients, an initial treatment exhibits a favorable response, whereas in most cases, later tumor recurrence or regrowth becomes a concern after radiation therapy. This is associated with the tumor radio-resistance. Therefore, analyzing the mechanisms of tumor radio-resistance is crucial for enhancing the treatment outcomes of radiation therapy. The aim of this study is to elucidate several mechanisms contributing to tumor radio-resistance in canine tumors focusing on programmed death ligand 1 (PD-L1) and JAK-STAT signaling pathway for the establishment of novel therapeutic strategies targeting these mechanisms to improve patient outcomes.

In Chapter I, to assess whether inflammatory signaling and DNA damage signaling is involved in programmed death ligand 1 (PD-L1) regulation in canine tumors and to elucidate the underlying mechanisms, the effects of interferon (IFN)-γ, tumor necrosis factor (TNF)-α treatment and X-irradiation exposure were evaluated in canine malignant melanoma cell lines (CMeC and LMeC) and an osteosarcoma cell line (HMPOS). The protein level of PD-L1 expression was increased on all tumor cells treated with IFN-γ and TNF-α, but not with X-irradiation. Upon IFN-γ stimulation, higher gene expression of PD-L1, signal transducer and activator of transcription (STAT)1, STAT3, and genes regulated by STAT activation was demonstrated in all cell lines. Upregulation of these genes was inhibited by the addition of a Janus kinase (JAK) inhibitor, oclacitinib. In contrast, upon TNF-α stimulation, all cell lines indicated an increase in expression of the nuclear factor κ B (NF-κB) gene RELA and genes regulated by NF-κB activation, whereas PD-L1 expression was upregulated in LMeC, but not in other cell lines. The addition of an NF-κB inhibitor, BAY 11-7082 suppressed the upregulated expression of these genes. PD-L1 upregulation induced by IFN-γ and TNF-α treatment was reduced by oclacitinib and BAY 11-7082, respectively, indicating that PD-L1 upregulation by IFN-γ and TNF-α stimulation is regulated via the JAK-STAT and NF-κB signaling pathways, respectively. These results provide insights into the role of inflammatory signaling in the regulation of PD-L1 in canine tumors.

In Chapter II, to establish a therapeutic approach targeting the JAK-STAT signaling pathway, the radio-sensitizing effect of oclacitinib in canine tumors and the

underlying mechanisms were assessed in osteosarcoma (HMPOS) and malignant melanoma (CMeC) cell lines. The radio-sensitizing effect of oclacitinib was evaluated using a clonogenic assay and a tumor growth assessment in a murine xenograft model (BALB/cAJcl-nu/nu). The protein levels of STAT3 and PARP through Western blotting were assessed, gene expressions regulated by STAT3 were examined using reverse-transcription quantitative polymerase chain reaction, and apoptosis and cell cycle were analyzed using flow cytometry. Oclacitinib significantly enhanced the radio-sensitivity of tumor cells both in vitro and in vivo. In cells exposed to X-irradiation, STAT3 expression was significantly activated in a dose- and time-dependent manner, which was effectively suppressed by oclacitinib. Oclacitinib significantly enhanced radiation-induced apoptosis by inhibiting the expression of anti-apoptosis genes (survivin, Bcl-XL, and MCL1) and PARP protein in HMPOS, but not in CMeC. Additionally, oclacitinib significantly inhibited the transcription of cell-cycle regulating genes (CCND1, Cyclin-dependent kinase 4 and 6) and arrested cell cycle progression from the G1 phase to subsequent phases. In conclusion, oclacitinib enhanced radio-sensitivity both in vitro and in vivo by triggering apoptosis and impeding cell cycle progression via STAT3 inhibition in canine tumor cell lines. This study suggested the clinical therapeutic potential of oclacitinib in combination with radiation therapy, aiming to enhance treatment efficacy and outcomes in dogs with tumors.

Taken together, several regulatory mechanisms of PD-L1 expression on canine tumors were elucidated. The JAK-STAT signaling pathway plays a pivotal role in the regulation of not only PD-L1 upregulation induced by IFN-γ but also the radio-sensitivity of canine tumors. In addition, oclacitinib targeting STAT3 was shown to be effective as a radio-sensitizer in canine tumors.

ACKNOWLEDGEMENT

I would like to express my deepest gratitude to my professors, Dr. Masahiro Okumura, Dr. Takafumi Sunaga, and Dr. Sangho Kim, in Laboratory of Veterinary Surgery, Department of Clinical Sciences, Graduate School of Veterinary Medicine, Hokkaido University (Sapporo, Japan), for their continuous mentoring, guidance, assistance, and encouragement throughout this work.

I would like to express my sincere appreciation to Dr. Kenji Hosoya, in Veterinary Teaching Hospital, Faculty of Veterinary Medicine, Hokkaido University, for their invaluable advice on the experiments and critical review on the manuscript.

I am deeply grateful Dr. Tatsuya Deguchi, in Department of Veterinary Medicine, School of Veterinary Medicine, Rakuno Gakuen University (Sapporo, Japan), for his mentoring, technical assistance, and valuable advice on the research.

I owe a deep debt of gratitude to Dr. Satoru Konnai, in Laboratory of Infectious Diseases, Department of Disease Control, Faculty of Veterinary Medicine, Hokkaido University, for his valuable advice on the research and critical review on the manuscript.

I greatly appreciate Dr. Naoya Maekawa and Dr. Tomohiro Okagawa, in Department of Advanced Pharmaceutics, Faculty of Veterinary Medicine, Hokkaido University, for their technical assistance and invaluable advice on the experiments.

I would like to extend my sincere gratitude to Dr. Mitsuyoshi Takiguchi, in Laboratory of Veterinary Internal Medicine, Department of Veterinary Clinical Sciences, Graduate School of Veterinary Medicine, Hokkaido University, for his critical review on the manuscript.

I greatly thank Dr. Osamu Inanami and Dr. Hironobu Yasui, in Laboratory of Radiation Biology, Department of Applied Veterinary Sciences, Graduate School of Veterinary Medicine, Hokkaido University, for their technical advice and assistance on the research.

I would like to extend my sincere condolences on the death of experimental animals that were used for my work.

I am very thankful to all members in Laboratory of Veterinary Surgery and Veterinary Teaching Hospital, Faculty of Veterinary Medicine, Hokkaido University, for their excellent help and warm friendship.

I would like to express my profound gratitude to my family and friends for their encouragement and support throughout my education and research.

Finally, I would like to thank all people who helped me to complete this study. Thank you so much.

REFERENCES

Akaraphutiporn E, Bwalya EC, Kim S, Sunaga T, Echigo R and Okumura M. Effects of pentosan polysulfate on cell proliferation, cell cycle progression and cyclin-dependent kinases expression in canine articular chondrocytes. J Vet Med Sci. **82(8)**, 1209–1218, 2020.

Akaraphutiporn E, Sunaga T, Bwalya EC, Yanlin W, Carol M and Okumura M. An insight into the role of apoptosis and autophagy in nitric oxide–induced articular chondrocyte cell death. Cartilage, **13(2)**, 826-838, 2021.

Amiri KI, and Richmond A. Role of nuclear factor-κB in melanoma. Cancer Metastasis Rev. **24(2)**, 301–313, 2005.

An JH, Li Q, Ryu MO, Nam AR, Bhang DH, Jung YC, Song WJ and Youn HY. TSG-6 in extracellular vesicles from canine mesenchymal stem/stromal is a major factor in relieving DSS-induced colitis. PLoS One, **15(2)**, e0220756, 2020.

Antonangeli F, Natalini A, Garassino MC, Sica A, Santoni A and di Rosa F. Regulation of PD-L1 expression by NF-κB in cancer. Front Immunol. **11**, 584626, 2020.

Antonia SJ, Villegas D, Daniel D, Vicente S, Murakami S, Hui R, Kurata T, Chiappori A, Lee KH, de Wit M, Cho BC, Bourhaba M, Quantin X, Tokito T, Mekhail T, Planchard D, Kim YC, Karapetis CS, Hiret S, Ostoros G, Kubota K, Gray JE, Paz-Ares L, de Castro Carpeno J, Faivre-Finn C, Reck M, Vansteenkiste J, Spigel DR, Wadsworth C, Melillo G, Taboada M, Dennis PA, and Ozguroglu M. Overall survival with durvalumab after chemoradiotherapy in stage III NSCLC. N Engl J Med. **379(24)**, 2342-2350, 2018

Ashrafizadeh M, Farhood B, Eleojo Musa A, Taeb S and Najafi, M. Damage-associated molecular patterns in tumor radiotherapy. Int Immunopharmacol. **86**, 106761, 2020.

Banerjee K and Resat H. Constitutive activation of STAT3 in breast cancer cells: A review. Int J Cancer. **138(11)**, 2570–2578, 2016.

Barrett LE, Gardner HL, Barber LG, Sadowski A and London CA. Safety and toxicity of combined oclacitinib and carboplatin or doxorubicin in dogs with solid tumors: A pilot study. BMC Vet Res. **15(1)**, 1-7, 2019.

Barroga EF, Kadosawa T, Okumura M and Fujinaga T. Establishment and characterization of the growth and pulmonary metastasis of a highly lung metastasizing cell line from canine osteosarcoma in nude mice. J Vet Med Sci. **61(4)**, 361-367, 1999.

Bertoli C, Skotheim JM and De Bruin RAM. Control of cell cycle transcription during G1 and S phases. Nat Rev Mol Cell Biol. **14(8)**, 518–528, 2013.

Bid HK, Oswald D, Li C, London CA, Lin J and Houghton PJ. Anti-angiogenic activity of a small molecule STAT3 inhibitor LLL12. PLoS One. **7(4)**, e35513, 2012.

Blank C, Gajewski TF and Mackensen A. Interaction of PD-L1 on tumor cells with PD-1 on tumor-specific T cells as a mechanism of immune evasion: Implications for tumor immunotherapy. Cancer Immunol Immunother. **54(4)**, 307–314, 2005.

Brahmer JR, Tykodi SS, Chow LQM, Hwu WJ, Topalian SL, Hwu P, Drake CG, Camacho LH, Kauh J, Odunsi K, Pitot HC, Hamid O, Bhatia S, Martins R, Eaton K, Chen S, Salay TM, Alaparthy S, Grosso JF, Korman AJ, Parker SM, Agrawal S, Goldberg SM, Pardoll DM, Gupta A and Wigginton JM. Safety and activity of anti–PD-L1 antibody in patients with advanced cancer. N Engl J Med. **366(26)**, 2455–2465, 2012.

Bwalya EC, Kim S, Fang J, Wijekoon HMS, Hosoya K and Okumura M. Pentosan polysulfate inhibits IL-1β-induced iNOS, c-Jun and HIF-1α upregulation in canine articular chondrocytes. PLoS One. **12(5)**, e0177144, 2017.

Carter L, Fouser LA, Jussif J, Fitz L, Deng B, Wood CR, Collins M, Honjo T, Freeman GJ and Carreno BM. PD-1:PD-L inhibitory pathway affects both CD4(+) and CD8(+) T cells and is overcome by IL-2. Eur J Immunol. **32(3)**, 634–643, 2002.

Chen M, Pockaj B, Andreozzi M, Barrett MT, Krishna S, Eaton S, Niu R and Anderson KS. JAK2 and PD-L1 amplification enhance the dynamic expression of PD-L1 in triple-negative breast cancer. Clin Breast Cancer. **18(5)**, 1205–1215, 2018.

Chen MF, Chen PT, Chen WC, Lu MS, Lin PY and Lee KD. The role of PD-L1 in the radiation response and prognosis for esophageal squamous cell carcinoma related to IL-6 and T-cell immunosuppression. Oncotarget. **7(7)**, 7913–7924, 2016.

Collard WT, Hummel BD, Fielder AF, King VL, Boucher JF, Mullins MA, Malpas PB and Stegemann MR. The pharmacokinetics of oclacitinib maleate, a Janus kinase inhibitor, in the dog. J Vet Pharmacol Ther. **37(3)**, 279–285, 2014.

Cosgrove SB, Cleaver DM, King VL, Gilmer AR, Daniels AE, Wren JA and Stegemann MR. Long-term compassionate use of oclacitinib in dogs with atopic and allergic skin disease: Safety, efficacy and quality of life. Vet Dermatol. **26(3)**, 171-179, 2015.

Couto JI, Bear MD, Lin J, Pennel M, Kulp SK, Kisseberth WC and London CA. Biologic activity of the novel small molecule STAT3 inhibitor LLL12 against canine osteosarcoma cell lines. BMC Vet Res. **8**, 244, 2012.

De Bruin T, De Rooster H, Van Bree H and Cox E. Interleukin-8 mRNA expression in synovial fluid of canine stifle joints with osteoarthritis. Vet Immunol Immunopathol. **108(3-4)**, 387–397, 2005.

Deguchi T, Maekawa N, Konnai S, Owaki R, Hosoya K, Morishita K, Nakamura M, Okagawa T, Takeuchi H, Kim S, Kinoshita R, Tachibana Y, Yokokawa M, Takagi S,

Kato Y, Suzuki Y, Murata S and Ohashi K. Enhanced systemic antitumour immunity by hypofractionated radiotherapy and anti-PD-L1 therapy in dogs with pulmonary metastatic oral malignant melanoma. Cancers. **15(11)**, 3013, 2023.

Dermani FK, Samadi P, Rahmani G, Kohlan AK and Najafi R. PD-1/PD-L1 immune checkpoint: Potential target for cancer therapy. J Cell Physiol. **234(2)**, 1313–1325, 2019.

Diaz N, Minton S, Cox C, Bowman T, Gritsko T, Garcia R, Eweis I, Wloch M, Livingston S, Seijo E, Cantor A, Lee JH, Beam CA, Sullivan D, Jove R and Muro-Cacho CA. Activation of Stat3 in primary tumors from high-risk breast cancer patients is associated with elevated levels of activated Src and survivin expression. Clin Cancer Res. **12(1)**, 20–28, 2006.

Dong H, Strome SE, Salomao DR, Tamura H, Hirano F, Flies DB, Roche PC, Lu J, Zhu G, Tamada K, Lennon VA, Cells E and Chen L. Tumor-associated B7-H1 promotes T-cell apoptosis: A potential mechanism of immune evasion. Nat Med. **8(8)**, 793–800, 2002.

Efstathiou JA, Spiegel DY, Shipley WU, Heney NM, Kaufman DS, Niemierko A, Coen JJ, Skowronski RY, Paly JJ, McGovern FJ and Zietman AL. Long-term outcomes of selective bladder preservation by combined-modality therapy for invasive bladder cancer: The MGH experience. Eur Urol. **61(4)**, 705–711, 2012.

Eto S, Yanai H, Hangai S, Kato D, Nishimura R and Nakagawa T. The impact of damage-associated molecules released from canine tumor cells on gene expression in macrophages. Sci Rep. **11(1)**, 8525, 2021.

Fossey SL, Liao AT, Mccleese JK, Bear MD, Lin J, Li P, Kisseberth WC and London CA. Characterization of STAT3 activation and expression in canine and human osteosarcoma. BMC Cancer. **9**, 81, 2009.

Fukuyama T, Ehling S, Cook E and Bäumer W. Topically administered janus-kinase

inhibitors tofacitinib and oclacitinib display impressive antipruritic and anti-inflammatory responses in a model of allergic dermatitis. J Pharmacol Exp Ther. **354(3)**, 394–405, 2015.

Gao L, Li FS, Chen XH, Liu QW, Feng JB, Liu QJ and Su X. Radiation induces phosphorylation of STAT3 in a dose- and time-dependent manner. Asian Pac J Cancer Prev. **15(15)**, 6161–6164, 2014.

Garcia R, Bowman TL, Niu G, Yu H, Minton S, Muro-Cacho CA, Cox CE, Falcone R, Fairclough R, Parsons S, Laudano A, Gazit A, Levitzki A, Kraker A and Jove R. Constitutive activation of Stat3 by the Src and JAK tyrosine kinases participates in growth regulation of human breast carcinoma cells. Oncogene. **20(20)**, 2499-2513, 2001.

Garcia-Diaz A, Shin DS, Moreno BH, Saco J, Escuin-Ordinas H, Rodriguez GA, Zaretsky JM, Sun L, Hugo W, Wang X, Parisi G, Saus CP, Torrejon DY, Graeber TG, Comin-Anduix B, Hu-Lieskovan S, Damoiseaux R, Lo RS and Ribas A. Interferon receptor signaling pathways regulating PD-L1 and PD-L2 expression. Cell Rep. **19(6)**, 1189–1201, 2017.

Gonzales AJ, Bowman JW, Fici GJ, Zhang M, Mann DW and Mitton-Fry M. Oclacitinib (APOQUEL®) is a novel Janus kinase inhibitor with activity against cytokines involved in allergy. J Vet Pharmacol Ther. **37(4)**, 317–324, 2014.

Hamid O, Robert C, Daud A, Hodi FS, Hwu WJ, Kefford R, Wolchok JD, Hersey P, Joseph RW, Weber JS, Dronca R, Gangadhar TC, Patnaik A, Zarour H, Joshua AM, Gergich K, Elassaiss-Schaap J, Algazi A, Mateus C, Boasberg P, Tumeh PC, Chmielowski B, Ebbinghaus SW, Nicole X, Kang P and Ribas A. Safety and tumor responses with lambrolizumab (Anti–PD-1) in melanoma. N Engl J Med. **369(2)**, 134–144, 2013.

Han JY, Woo Nam S, Han J, Kim JIL, Heon Park S, Hyun Cho S, Han NI, Yang JM, Kim JK, Choi SW, Lee YS, Chung KW and Sun HS. Spontaneous regression of a large

hepatocellular carcinoma with skull metastasis. J Gastroenterol Hepatol. **20(3)**, 488–492, 2005.

Hartley G, Faulhaber E, Caldwell A, Coy J, Kurihara J, Guth A, Regan D and Dow S. Immune regulation of canine tumour and macrophage PD-L1 expression. Vet Comp Oncol. **15(2)**, 534–549, 2017.

Hayden MS and Ghosh S. Shared principles in NF-κB signaling. Cell. **132**, 344–362, 2008.

Hino R, Kabashima K, Kato Y, Yagi H, Nakamura M, Honjo T, Okazaki T and Tokura Y. Tumor cell expression of programmed cell death-1 ligand 1 is a prognostic factor for malignant melanoma. Cancer. **116(7)**, 1757–1766, 2010.

Hou J, Schindler U, Henzel WJ, Ho TC, Brasseur M and McKnight SL. An interleukin-4-induced transcription factor: IL-4 Stat. Science. **265(5179)**, 1701–1706, 1994.

Hydbring P, Malumbres M and Sicinski P. Non-canonical functions of cell cycle cyclins and cyclin-dependent kinases. Nat Rev Mol Cell Biol. **17(5)**, 280–292, 2016.

Igase M, Nemoto Y, Itamoto K, Tani K, Nakaichi M, Sakurai M, Sakai Y, Noguchi S, Kato M, Tsukui T and Mizuno T. A pilot clinical study of the therapeutic antibody against canine PD-1 for advanced spontaneous cancers in dogs. Sci Rep. **10(1)**, 18311, 2020.

Ikeda S, Okamoto T, Okano S, Umemoto Y, Tagawa T, Morodomi Y, Kohno M, Shimamatsu S, Kitahara H, Suzuki Y, Fujishita T and Maehara Y. PD-L1 is upregulated by simultaneous amplification of the PD-L1 and JAK2 genes in non-small cell lung cancer. J Thorac Oncol. **11(1)**, 62–71, 2016.

Im H, Lee J, Lee HJ, Kim DY, Kim EJ and Yi JY. Cyclin D1 promotes radio-resistance

through regulation of RAD51 in melanoma. Exp Dermatol. **32(10)**, 1706–1716, 2023

Inoue K, Ohashi E, Kadosawa T, Hong SH, Matsunaga S, Mochizuki M, Nishimura R and Sasaki N. Establishment and characterization of four canine melanoma cell lines. J Vet Med Sci. **66(11)**, 1437-1440, 2004.

Iwai Y, Hamanishi J, Chamoto K and Honjo T. Cancer immunotherapies targeting the PD-1 signaling pathway. J Biomed Sci. **24(26)**, 26, 2017.

Iwasa T, Okamoto I, Suzuki M, Nakahara T, Yamanaka K, Hatashita E, Yamada Y, Fukuoka M, Ono K and Nakagawa K. Radiosensitizing effect of YM155, a novel small-molecule survivin suppressant, in non-small cell lung cancer cell lines. Clin Cancer Res. **14(20)**, 6496–6504, 2008.

Jenkins RW, Barbie DA and Flaherty KT. Mechanisms of resistance to immune checkpoint inhibitors. Br J Cancer. **118(1)**, 9–16, 2018.

Jeong EG, Kim MS, Nam HK, Min CK, Lee S, Chung YJ, Yoo NJ and Lee SH. Somatic mutations of JAK1 and JAK3 in acute leukemias and solid cancers. Clin Cancer Res. **14(12)**, 3716–3721, 2008.

Jorgovanovic D, Song M, Wang L and Zhang Y. Roles of IFN-γ in tumor progression and regression: A review. Biomark Res. **8**, 49, 2020.

Katsuki S, Takahashi Y, Tamari K, Minami K, Takenaka W, Ibuki Y, Yamamoto J, Tatekawa S, Hayashi K, Seo Y, Isohashi F, Ogawa K and Koizumi M. Radiation therapy enhances systemic antitumor efficacy in PD-L1 therapy regardless of sequence of radiation in murine osteosarcoma. PLoS One. **17(7)**, e0271205, 2022.

Kondo A, Yamashita T, Tamura H, Zhao W, Tsuji T, Shimizu M, Shinya E, Takahashi H, Tamada K, Chen L, Dan K and Ogata K. Interferon-γ and tumor necrosis factor-α induce an immunoinhibitory molecule, B7-H1, via nuclear factor-κB activation

in blasts in myelodysplastic syndromes. Blood. **116(7)**, 1124–1131, 2010.

Król M, Pawłowski KM, Dolka I, Musielak O, Majchrzak K, Mucha J, and Motyl T. Density of Gr1-positive myeloid precursor cells, p-STAT3 expression and gene expression pattern in canine mammary cancer metastasis. Vet Res Commun. **35(7)**, 409–423, 2011.

Krolewski JJ, Lee R, Eddy R, Shows TB and Dalla-Favera R. Identification and chromosomal mapping of new human tyrosine kinase genes. Oncogene. **5(3)**, 277–282, 1990.

Kulesza DW, Ramji K, Maleszewska M, Mieczkowski J, Dabrowski M, Chouaib S and Kaminska B. Search for novel STAT3-dependent genes reveals SERPINA3 as a new STAT3 target that regulates invasion of human melanoma cells. Lab Invest. **99(11)**, 1607–1621, 2019.

Kumar SR, Kim DY, Henry CJ, Bryan JN, Robinson KL and Eaton AM. Programmed death ligand 1 is expressed in canine B cell lymphoma and downregulated by MEK inhibitors. Vet Comp Oncol. **15(4)**, 1527–1536, 2017.

Laha D, Grant R, Mishra P and Nilubol N. The role of tumor necrosis factor in manipulating the immunological response of tumor microenvironment. Front Immunol. **12,** 656908, 2021.

Langley R, Bump E, Quartuccio S, Medeiros D and Braunhut S. Radiation-induced apoptosis in microvascular endothelial cells. Br J Cancer. **75(5)**, 666–672, 1997.

Lau J, Ilkhanizadeh S, Wang S, Miroshnikova YA, Salvatierra NA, Wong RA, Schmidt C, Weaver VM, Weiss WA and Persson AI. STAT3 blockade inhibits radiation-induced malignant progression in glioma. Cancer Res. **75(20)**, 4302–4311, 2015.

Li F, Gao L, Wang Z, Dong B, Yan T, Jiang Q and Chen X. Radiation enhances the invasion abilities of pulmonary adenocarcinoma cells via STAT3. Mol Med Rep. **7(6)**, 1883–1888, 2013.

Li P, Wang J, Chen G, Zhang X, Lin D, Zhou Y, Yu Y, Liu W and Zhang D. Oncolytic activity of canine distemper virus in canine mammary tubular adenocarcinoma cells. Vet Comp Oncol. **17(2)**, 174–183, 2019.

Licursi V, Anzellotti S, Favaro J, Sineri S, Carucci N, Cundari E, Fiore M, Guarguaglini G, Pippa S, Nisi PS, Vernì F, Biagioni S, Cacci E, Amendola R, Lupo G and Negri R. X-ray irradiated cultures of mouse cortical neural stem/progenitor cells recover cell viability and proliferation with dose-dependent kinetics. Sci Rep. **10(1)**, 6562, 2020.

Lim SO, Li CW, Xia W, Cha JH, Chan LC, Wu Y, Chang SS, Lin WC, Hsu JM, Hsu YH, Kim T, Chang WC, Hsu JL, Yamaguchi H, Ding Q, Wang Y, Yang Y, Chen CH, Sahin AA, Yu D, Hortobagyi GN and Hung MC. Deubiquitination and stabilization of PD-L1 by CSN5. Cancer Cell. **30(6)**, 925–939, 2016.

Liu IL, Chung TF, Huang WH, Hsu CH, Liu CC, Chiu YH, Huang KC, Liao ATC and Lin CS. Kynurenine 3-monooxygenase (KMO), and signal transducer and activator of transcription 3 (STAT3) expression is involved in tumour proliferation and predicts poor survival in canine melanoma. Vet Comp Oncol. **19(1)**, 79–91, 2021.

Liu J, Hamrouni A, Wolowiec D, Coiteux V, Kuliczkowski K, Hetuin D, Saudemont A and Quesnel B. Plasma cells from multiple myeloma patients express B7-H1 (PD-L1) and increase expression after stimulation with IFN-γ and TLR ligands via a MyD88-, TRAF6-, and MEK-dependent pathway. Blood. **110(1)**, 296–304, 2007.

Liu S, Imani S, Deng Y, Pathak JL, Wen Q, Chen Y and Wu J. Targeting IFN/STAT1 pathway as a promising strategy to overcome radio-resistance. OncoTargets Ther. **13**, 6037–6050, 2020.

Liu X, Robinson GW, Gouilleux F, Groner B and Hennighausen L. Cloning and expression of Stat5 and an additional homologue (Stat5b) involved in prolactin signal transduction in mouse mammary tissue. Proc Nat Acad Sci USA. **92(19)**, 8831–8835, 1995.

Liu X, Robinson GW, Wagner KU, Garrett L, Wynshaw-Boris A and Hennighausen L. Stat5a is mandatory for adult mammary gland development and lactogenesis. Genes Dev. **11(2)**, 179–186, 1997.

Lo HW, Cao X, Zhu H and Ali-Osman F. Constitutively activated STAT3 frequently coexpresses with epidermal growth factor receptor in high-grade gliomas and targeting STAT3 sensitizes them to iressa and alkylators. Clin Cancer Res. **14(19)**, 6042–6054, 2008.

Lu B, Mu Y, Cao C, Zeng F, Schneider S, Tan J, Price J, Chen J, Freeman M and Hallahan DE. Survivin as a therapeutic target for radiation sensitization in lung cancer. Cancer Res. **64(8)**, 2840–2845, 2004.

Lu L, Dong J, Wang L, Xia Q, Zhang D, Kim H, Yin T, Fan S and Shen Q. Activation of STAT3 and Bcl-2 and reduction of reactive oxygen species (ROS) promote radio-resistance in breast cancer and overcome of radio-resistance with niclosamide. Oncogene. **37(39)**, 5292–5304, 2018.

Lu Z, Hong CC, Jark PC, Assumpção ALFV, Bollig N, Kong G and Pan X. JAK1/2 Inhibitors AZD1480 and CYT387 inhibit canine B-cell lymphoma growth by increasing apoptosis and disrupting cell proliferation. J Vet Int Med. **31(6)**, 1804–1815 2017.

Maekawa N, Konnai S, Ikebuchi R, Okagawa T, Adachi M, Takagi S, Kagawa Y, Nakajima C, Suzuki Y, Murata S and Ohashi K. Expression of PD-L1 on canine tumor cells and enhancement of IFN-γ production from tumor-infiltrating cells by PD-L1 blockade. PLoS One. **9(6)**, e98415, 2014.

Maekawa N, Konnai S, Okagawa T, Nishimori A, Ikebuchi R, Izumi Y, Takagi S, Kagawa Y, Nakajima C, Suzuki Y, Kato Y, Murata S and Ohashi K. Immunohistochemical analysis of PD-L1 expression in canine malignant cancers and PD-1 expression on lymphocytes in canine oral melanoma. PLoS One. **11(6)**, e0157176, 2016.

Maekawa N, Konnai S, Takagi S, Kagawa Y, Okagawa T, Nishimori A, Ikebuchi R, Izumi Y, Deguchi T, Nakajima C, Kato Y, Yamamoto K, Uemura H, Suzuki Y, Murata S and Ohashi K. A canine chimeric monoclonal antibody targeting PD-L1 and its clinical efficacy in canine oral malignant melanoma or undifferentiated sarcoma. Sci Rep., **7(1)**, 8951, 2017.

Maekawa N, Konnai S, Hosoya K, Kim S, Kinoshita R, Deguchi T, Owaki R, Tachibana Y, Yokokawa M, Takeuchi H, Kagawa Y, Takagi S, Ohta H, Kato Y, Yamamoto S, Yamamoto K, Suzuki Y, Okagawa T, Murata S and Ohashi K. Safety and clinical efficacy of an anti-PD-L1 antibody (c4G12) in dogs with advanced malignant tumours. PLoS One. **18(10)**, e0291727, 2023.

Moon JW, Kong SK, Kim BS, Kim HJ, Lim H, Noh K, Kim Y, Choi JW, Lee JH and Kim YS. IFNγ induces PD-L1 overexpression by JAK2/STAT1/IRF-1 signaling in EBV-positive gastric carcinoma. Sci Rep. **7(1)**, 17810, 2017.

Mora LB, Buettner R, Seigne J, Diaz J, Ahmad N, Garcia R, Bowman T, Falcone R, Fairclough R, Cantor A, Muro-Cacho C, Livingston S, Karras J, Pow-Sang J and Jove R. Constitutive activation of Stat3 in human prostate tumors and cell lines: direct inhibition of Stat3 signaling induces apoptosis of prostate cancer cells. Cancer Res. **62(22)**, 6659–6666, 2002.

Muenst S, Schaerli AR, Gao F, Däster S, Trella E, Droeser RA, Muraro MG, Zajac P, Zanetti R, Gillanders WE, Weber WP and Soysal SD. Expression of programmed death ligand 1 (PD-L1) is associated with poor prognosis in human breast cancer. Breast Cancer Res Treat. **146(1)**, 15–24, 2014.

Ni XY, Sui HX, Liu Y, Ke SZ, Wang YN and Gao FG. TGF-β of lung cancer microenvironment upregulates B7H1 and GITRL expression in dendritic cells and is associated with regulatory T cell generation. Oncol Rep. **28(2)**, 615–621, 2012.

Nishumura H and Honjo T. PD-1: an inhibitory immunoreceptor involved in peripheral tolerance. Trends Immunol. **22(5)**, 265–268, 2001.

Nolan MW, Kogan L, Griffin LR, Custis JT, Harmon JF, Biller BJ and LaRue SM. Intensity-modulated and image-guided radiation therapy for treatment of genitourinary carcinomas in dogs. J Vet Intern Med. **26(4)**, 987–995, 2012.

Pan L, Zhang R, Ma L, Pierson CR, Finlay JL, Li C and Lin J. STAT3 inhibitor in combination with irradiation significantly inhibits cell viability, cell migration, invasion and tumorsphere growth of human medulloblastoma cells. Cancer Biol Ther. **22(7-9)**, 430–439, 2021.

Park SS, Dong H, Liu X, Harrington SM, Krco CJ, Grams MP, Mansfield AS, Furutani KM, Olivier KR and Kwon ED. PD-1 Restrains Radiotherapy-Induced Abscopal Effect. Cancer Immunol Res. **3(6)**, 610-619, 2015.

Peters IR, Helps CR, Calvert EL, Hall EJ and Day MJ. Cytokine mRNA quantification in histologically normal canine duodenal mucosa by real-time RT-PCR. Vet Immunol Immunopathol. **103(1-2)**, 101–111, 2005.

Pitroda SP, Stack ME, Liu GF, Song SS, Chen L, Liang H, Parekh AD, Huang X, Roach P, Posner MC, Weichselbaum RR and Khodarev NN. JAK2 inhibitor sar302503 abrogates pd-l1 expression and targets therapy-resistant non–small cell lung cancers. Mol Cancer Ther. **17(4)**, 732–739, 2018.

Quandt D, Jasinski-Bergner S, Müller U, Schulze B and Seliger B. Synergistic effects of IL-4 and TNFα on the induction of B7-H1 in renal cell carcinoma cells inhibiting

allogeneic T cell proliferation. J Transl Med. **12(1)**, 151, 2014.

Ren Y, Yang P, Li C, Wang W, Zhang T, Li J, Li H, Dong C, Meng W and Zhou H. Ionizing radiation triggers mitophagy to enhance DNA damage in cancer cells. Cell Death Discov. **9(1)**, 267, 2023.

Sano J, Oguma K, Kano R, Yazawa M, Tsujimoto H and Hasegawa A. High expression of Bcl-xL in delayed apoptosis of canine neutrophils induced by lipopolysaccharide. Res Vet Sci. **78(2)**, 183–187, 2005.

Sato H, Niimi A, Yasuhara T, Permata TBM, Hagiwara Y, Isono M, Nuryadi E, Sekine R, Oike T, Kakoti S, Yoshimoto Y, Held KD, Suzuki Y, Kono K, Miyagawa K, Nakano T and Shibata A. DNA double-strand break repair pathway regulates PD-L1 expression in cancer cells. Nat Commun. **8(1)**, 1751, 2017.

Schroder K, Hertzog PJ, Ravasi T and Hume DA. Interferon-γ: an overview of signals, mechanisms, and functions. J Leukoc Biol. **75(2)**, 163–189, 2004.

Strome SE, Dong H, Tamura H, Voss SG, Flies DB, Tamada K, Salomao D, Cheville J, Hirano F, Lin W, Kasperbauer JL, Ballman KV and Chen L. B7-H1 blockade augments adoptive T-cell immunotherapy for squamous cell carcinoma. Cancer Res. **63(19)**, 6501–6505, 2003.

Sharma P, Hu-Lieskovan S, Wargo JA and Ribas A. Primary, adaptive, and acquired resistance to cancer immunotherapy. Cell. **168(4)**, 707–723, 2017.

Shuai K, Horvath CM, Huang LHT, Qureshi SA, Cowburn D and Darnell JE. Interferon activation of the transcription factor Stat91 involves dimerization through SH2-phosphotyrosyl peptide interactions. Cell. **76(5)**, 821–828, 1994.

Shuai K, Stark GR, Kerr LM and Darnell JE. A Single Phosphotyrosine residue of stat91 required for gene activation by interferon-γ. Science. **261(5129)**, 1744–1746, 1993.

Singh-Gupta V, Zhang H, Banerjee S, Kong D, Raffoul JJ, Sarkar FH and Hillman GG. Radiation-induced HIF-1α cell survival pathway is inhibited by soy isoflavones in prostate cancer cells. Int J Cancer. **124(7)**, 1675–1684, 2009.

Stephanou A, Brar BK, Knight RA and Latchman DS. Opposing actions of STAT-1 and STAT-3 on the Bcl-2 and Bcl-x promoters. Cell Death Differ. **7(3)**, 329–330, 2000.

Steven H, Lu W, Bevan M, Peter FT, Wayne LH, Stephen GS, Jaffer AA, James DC, Ritsuko K and Zhongxing L. Propensity score-based comparison of long-term outcomes with 3-dimensional conformal radiotherapy vs intensity-modulated radiotherapy for esophageal cancer. Int J Radiat Oncol Biol Phys. **84(5)**, 1078-1085, 2012.

Sun Y, Moretti L, Giacalone NJ, Schleicher S, Speirs CK, Carbone DP and Lu B. Inhibition of JAK2 signaling by TG101209 enhances radiotherapy in lung cancer models. J Thorac Oncol. **6(4)**, 699–706, 2011.

Sung K, Hosoya K, Murase Y, Deguchi T, Kim S, Sunaga T and Okumura M. Visualizing the cancer stem-like properties of canine tumour cells with low proteasome activity. Vet Comp Oncol. **20(1)**, 324–335, 2022.

Takeuchi H, Konnai S, Maekawa N, Minato E, Ichikawa Y, Kobayashi A, Okagawa T, Murata S and Ohashi K. Expression analysis of canine CMTM6 and CMTM4 as potential regulators of the PD-L1 protein in canine cancers. Front Vet Sci. **7**, 330, 2020.

Theelen WSME, Peulen HMU, Lalezari F, van der Noort V, de Vries JF, Aerts JGJV, Dumoulin DW, Bahce I, Niemeijer AN, de Lange AJ, Monkhorst K and Baas P. Effect of pembrolizumab after stereotactic body radiotherapy vs pembrolizumab alone on tumor response in patients with advanced non–small cell lung cancer. JAMA Oncol. **5(9)**, 1276-1282, 2019.

Vascellari M, Giantin M, Capello K, Carminato A, Morello EM, Vercelli A, Granato

A, Buracco P, Dacasto M and Mutinelli F. Expression of Ki67, BCL-2, and COX-2 in canine cutaneous mast cell tumors: Association With Grading and Prognosis. Vet Pathol. **50(1)**, 110–121, 2013.

Wang F, Ma X, Mao G, Zhang X and Kong Z. STAT3 enhances radiation-induced tumor migration, invasion and stem-like properties of bladder cancer. Mol Med Rep. **23(1)**, 1–10, 2021.

Wang M, Sun X, Xin H, Wen Z and Cheng Y. SPP1 promotes radiation resistance through JAK2/STAT3 pathway in esophageal carcinoma. Cancer Med. **11(23)**, 4526–4543, 2022.

Wang T, Niu G, Kortylewski M, Burdelya L, Shain K, Zhang S, Bhattacharya R, Gabrilovich D, Heller R, Coppola D, Dalton W, Jove R, Pardoll D and Yu H. Regulation of the innate and adaptive immune responses by Stat-3 signaling in tumor cells. Nat Med. **10(1)**, 48–54, 2004.

Wang X, Goldstein D, Crowe PJ and Yang JL. Impact of STAT3 inhibition on survival of osteosarcoma cell lines. Anticancer Res. **34(11)**, 6537–6545, 2014.

Wang X, Yang L, Huang F, Zhang Q, Liu S, Ma L and You Z. Inflammatory cytokines IL-17 and TNF-α up-regulate PD-L1 expression in human prostate and colon cancer cells. Immunol Lett. **184**, 7–14 2017.

Wang Y, Mwale C, Akaraphutiporn E, Kim S, Sunaga T and Okumura M. Sulfate level relied effects of pentosan polysulfate sodium on inhibiting the proliferationof canine articular chondrocytes by targeting PI3K/Akt pathway. Japanese Journal of Veterinary Research. **71(2)**, 35-47, 2023.

Wei J, Montalvo-Ortiz W, Yu L, Krasco A, Ebstein S, Cortez C, Lowy I, Murphy AJ, Sleeman MA and Skokos D. Sequence of αPD-1 relative to local tumor irradiation determines the induction of abscopalantitumor immune responses. Sci Immunol. **6(58)**,

eabg0117, 2021.

Wilks AF, Harpur AG, Kurban RR, Ralph SJ, Zurcher G and Ziemiecki A. Two novel protein-tyrosine kinases, each with a second phosphotransferase-related catalytic domain, define a new class of protein kinase. Mol Cell Biol. **11(4)**, 2057–2065, 1991.

Wilson H, Huelsmeyer M, Chun R, Young KM, Friedrichs K and Argyle DJ. Isolation and characterisation of cancer stem cells from canine osteosarcoma. Vet J. **175(1)**, 69–75, 2008.

Wu CT, Chen WC, Chang YH, Lin WY and Chen MF. The role of PD-L1 in the radiation response and clinical outcome for bladder cancer. Sci Rep. **6**, 19740, 2016.

Xu LJ, Chen XD, Shen MJ, Yang DR, Fang L, Weng G, Tsai Y, Keng PC, Chen Y and Lee SO. Inhibition of IL-6-JAK/Stat3 signaling in castration-resistant prostate cancer cells enhances the NK cell-mediated cytotoxicity via alteration of PD-L1/NKG2D ligand levels. Mol Oncol. **12(3)**, 269–286, 2018.

Yan S, Li Z and Thiele CJ. Inhibition of STAT3 with orally active JAK inhibitor, AZD1480, decreases tumor growth in Neuroblastoma and Pediatric Sarcomas In vitro and In vivo. Oncotarget. **4(3)**, 433-445, 2013.

Yi M, Niu M, Xu L, Luo S and Wu K. Regulation of PD-L1 expression in the tumor microenvironment. J Hematol Oncol. **14(1)**, 10, 2021.

Zaretsky JM, Garcia-Diaz A, Shin DS, Escuin-Ordinas H, Hugo W, Hu-Lieskovan S, Torrejon DY, Abril-Rodriguez G, Sandoval S, Barthly L, Saco J, Moreno BH, Mezzadra R, Chmielowski B, Ruchalski K, Shintaku IP, Sanchez PJ, Puig-Saus C, Cherry G, Seja E, Kong X, Pang J, Berent-Maoz B, Comin-Anduix B, Graeber TG, Tumeh PC, Schumacher TNM, Lo RS and Ribas A. Mutations associated with acquired resistance to PD-1 blockade in melanoma. N Engl J Med. **375(9)**, 819–829, 2016.

Zhang Q, Zhou XM, Wei SZ, Cui DS, Deng KL, Liang G, Luo Y, Luo B and Liang XJ. STAT3 as a target for sensitizing prostate cancer cells to irradiation. J Radiat Res. **63(2)**, 174–182, 2022.

Zhang X, Wang X, Xu R, Ji J, Xu Y, Han M, Wei Y, Huang B, Chen A, Zhang Q, Li W, Wang J, Li X and Qiu C. YM155 decreases radiation-induced invasion and reverses epithelial-mesenchymal transition by targeting STAT3 in glioblastoma. J Transl Med. **16(1)**, 79, 2018.

Zhong Z, Wen Z and Darnell JE. Stat3 and Stat4: members of the family of signal transducers and activators of transcription. Proc Natl Acad Sci USA. **91(11)**, 4806–4810, 1994.

Zorzi E and Bonvini P. Inducible Hsp70 in the regulation of cancer cell survival: Analysis of chaperone induction, expression and activity. Cancers. **3(4)**, 3921–3956, 2011.

SUMMARY IN JAPANESE
和文要旨

医療、獣医療において腫瘍に対する放射線治療は重要かつ有効な治療法である。放射線治療を受けたほとんどの患者で、初期は良好な治療反応を示し、腫瘍の縮小や臨床症状の改善を認める。しかし、根治に至ることは稀であり、いずれは腫瘍の再増大を認め、死に至ることが問題となっている。この放射線治療後の腫瘍の再増大は、腫瘍の放射線治療抵抗性に起因していると考えられる。そのため、腫瘍における放射線治療抵抗性の発生機序を解析し、それらを標的とした新規治療戦略の確立が望まれている。

放射線治療は、腫瘍細胞に対する DNA 傷害作用のみならず、腫瘍細胞と周囲の間質により構成される腫瘍微小環境において T 細胞を活性化し、抗腫瘍効果を示す。しかし、ヒトおよびイヌの様々な腫瘍において、Programmed death ligand 1 (PD-L1)が高率に発現し、活性化 T 細胞上の Programmed death 1 (PD-1)と結合することで免疫回避を起こすことが報告されている。それに対し PD-1/PD-L1 経路の阻害と放射線治療の併用療法は、放射線治療の抗腫瘍効果を増強し、治療成績の向上を示した。そのため、腫瘍細胞における PD-L1 発現の抑制は放射線治療抵抗性腫瘍に対する有効な治療戦略であると考えられる。放射線照射により誘導される腫瘍細胞上の PD-L1 発現には、Janus kinase (JAK)-signal transducer and activator of transcription (STAT)シグナル伝達経路が重要な役割を果たすことと報告されている。一方で、イヌ腫瘍における PD-L1 発現機序は不明であり、その解明は新しい治療標的を探索する上で非常に重要である。

JAK-STAT シグナル伝達経路の中で、特に STAT3 の活性化は腫瘍進行を促進する因子として認識されている。放射線照射と JAK、あるいは STAT3 阻害剤を併用することで、腫瘍増殖抑制効果の増強が報告されている。そのため、JAK-STAT シグナル伝達経路の制御は腫瘍の放射線治療抵抗性に対する有効な治療戦略であると考えられる。そこで本研究では、イヌ腫瘍の放射線治療抵抗性の原因として、PD-L1 発現と JAK-STAT シグナル伝達経路に着目し、PD-L1 発現増強機序の解明、および放射線照射が JAK-STAT シグナル伝達経路に与える影響を解析した後、それらを治療の標的とすることで、がんの治療成績の向上および新規治療の発展に寄与することを最終目的とした。

第 1 章では、イヌ腫瘍における炎症性サイトカインおよび DNA 損傷と PD-L1 発現との関連性、ならびにその発現機序を明らかにするため、イヌの骨肉腫細胞株 (HMPOS)および悪性黒色腫細胞株 (CMeC、LMeC)を用いて、Interferon (IFN)-γ、Tumor necrosis factor (TNF)-α および放射線照射が細胞に与える影響を評価した。まず IFN-γ または TNF-

α を添加した全ての細胞で PD-L1 発現の上昇を認めた一方で、放射線照射では発現上昇は認めなかった。続いて IFN-γ 添加により、全ての細胞株で *PD-L1*、*STAT1*、*STAT3*、および STAT の下流の遺伝子の発現上昇を認め、その遺伝子発現上昇は、JAK 阻害剤であるオクラシチニブにより抑制された。一方で TNF-α 添加においては、全ての細胞株で *nuclear factor kappa B (NF-κB) gene RELA (RELA)*および *RELA* により制御される遺伝子の発現が上昇したものの、*PD-L1* 遺伝子の発現上昇は LMeC でのみ認めた。それらの発現上昇は、NF-κB 阻害剤である BAY11-7082 により抑制された。最後に IFN-γ および TNF-α 刺激により増強した PD-L1 発現は、それぞれオクラシチニブおよび BAY11-7082 の添加により抑制された。これらの結果から、イヌ腫瘍において、IFN-γ および TNF-α は、それぞれ JAK-STAT シグナル伝達経路および NF-κB シグナル伝達経路を介して PD-L1 発現を制御することが示された。さらに、イヌ腫瘍において放射線照射による PD-L1 発現増強には、放射線照射による DNA 損傷シグナルと比較し、炎症性シグナルがより重要な役割を果たしていることが示唆された。

第 2 章では、イヌ腫瘍における JAK-STAT シグナル伝達経路を標的とした治療の確立のため、オクラシチニブの放射線増感効果とその作用機序を解析することを目的とした。JAK 阻害薬であるオクラシチニブは、イヌのアトピー性皮膚炎およびアレルギー性皮膚炎に起因した痒みに対する治療薬であり、すでにイヌにおいて長期投与の安全性が報告されている。しかし、これまでイヌ腫瘍におけるオクラシチニブの抗腫瘍効果は明らかにされていない。そこで、イヌ骨肉腫細胞株（HMPOS）および悪性黒色腫細胞株（CMeC）を用いて、以下を検証した。まずオクラシチニブの放射線増感効果の有無について、コロニー形成法を用いた X 線暴露後の細胞生存率、および免疫不全マウス（BALB/cAJcl-nu/nu）を用いたイヌ腫瘍細胞由来の異種移植モデルにおける腫瘍体積の変化を評価したところ、双方においてオクラシチニブによる腫瘍細胞および腫瘍の放射線感受性の増加を認めた。放射線暴露後の細胞では、照射線量および時間依存性に STAT3 の活性化を認め、オクラシチニブの添加によりその活性化は抑制された。また HMPOS においてオクラシチニブは *Survivin*、*B cell lymphoma-extra large* および *myeloid cell leukemia 1* といった抗アポトーシス遺伝子発現に対する抑制作用、および Poly (ADP-ribose) polymerase (PARP)の活性化を増強する作用を示し、放射線によるアポトーシス誘導を増強した。さらに細胞周期解析において、全ての細胞株において *CCND1*、*cyclin-dependent kinase* (*CDK*)*4* および *CDK6* の遺伝子発現を抑制し、細胞周期解析において G1 期での細胞周期停止が起こることを示した。これらのことから、オクラシチニブはイヌ腫瘍に対し、STAT3 の活性化を抑制し、アポトーシス誘導および細胞周期停止を引

き起こすことで放射線増感効果を示すことが証明された。また放射線治療とオクラシチニブの併用療法によりイヌ腫瘍の治療成績が向上する可能性が示唆された。

本研究より、イヌ腫瘍における PD-L1 発現機序の一部が解明された。また JAK-STAT シグナル伝達経路は IFN-γ により誘導される PD-L1 発現に関わるだけでなく、STAT3 を介し腫瘍の放射線感受性に関わることが強く示され、STAT3 を標的としたオクラシチニブは、イヌ腫瘍における放射線増感薬として有効であることが示唆された。

ABSTRACT

Radiation therapy is a valuable treatment modality for cancer patients in both human beings and animals. In many patients, an initial course of radiation would exhibit a favorable response, whereas in most cases, the regrowth of tumor mass becomes a concern after radiation therapy. The regrowth of tumors after radiation therapy is thought to be due to complex mechanisms of it. Elucidating the mechanisms of tumor radio-resistance is required to establish a novel therapeutic strategy targeting the mechanisms of tumor radio-resistance.

The cytotoxic stress induced by radiation therapy activates T cell-mediating immune response in the tumor microenvironment (TME), leading to an effective antitumor response, but the expression of programmed death ligand 1 (PD-L1) on tumor cells, which is the ligand of programmed death 1 (PD-1) expressed on T cells, provides an immune evasion by suppressing cytotoxic T cells. Blockade of PD-1/PD-L1 axis in combination with radiation therapy enhanced antitumor effects of radiotherapy and improved treatment outcomes, indicating that the regulation of PD-L1 on tumor cells plays a pivotal role in overcoming tumor radio-resistance. Several regulatory mechanisms of PD-L1 expression have been shown in human tumors, however, little is known in canine tumors. In TME of human tumors, The Janus kinase (JAK)-signal transducer and activator of transcription (STAT) signaling pathway plays a key role in PD-L1 regulatory signaling.

Among JAK-STAT signaling pathways, STAT3 activation is well-known for its role in facilitating tumor growth. Irradiation in combination with JAK or STAT3 inhibitor enhanced radio-sensitivity and induced tumor growth delay in mice xenograft model of human cancer cells. Hence, Modulating the JAK-STAT signaling pathway may serve as an effective treatment strategy for overcoming tumor radio-resistance. The aim of this study is to elucidate the regulatory mechanisms contributing to tumor radio-resistance in canine tumors focusing on PD-L1 and JAK-STAT signaling pathway, and to investigate the radio-sensitizing effects of oclacitinib, an orally available JAK inhibitor in dogs, for the establishment of novel therapeutic strategies targeting these mechanisms to improve patient outcomes.

In Chapter I, to assess whether inflammatory signaling and DNA damage

signaling are involved in PD-L1 regulation in canine tumors and elucidate the underlying mechanisms, the effects of interferon (IFN)-γ and tumor necrosis factor (TNF)-α treatment and X-irradiation exposure were evaluated in two canine malignant melanoma cell lines (CMeC and LMeC) and an osteosarcoma cell line (HMPOS). The protein level of PD-L1 expression was increased on all tumor cells treated with IFN-γ and TNF-α, but not with X-irradiation. Upon IFN-γ stimulation, higher gene expression of PD-L1, STAT1, STAT3, and genes regulated by STAT activation was demonstrated in all cell lines. Upregulation of these genes was inhibited by the addition of a JAK inhibitor, oclacitinib. In contrast, upon TNF-α stimulation, all cell lines indicated an increase in expression of the nuclear factor kappa B (NF-κB) gene (RELA) and genes regulated by NF-κB activation, whereas PD-L1 expression was upregulated in LMeC only. The addition of an NF-κB inhibitor, BAY 11-7082 suppressed the upregulated expression of these genes. The upregulation of PD-L1 expression induced by IFN-γ and TNF-α treatment was reduced by oclacitinib and BAY 11-7082, respectively, indicating that PD-L1 upregulation by IFN-γ and TNF-α stimulation is regulated via the JAK-STAT and NF-κB signaling pathways, respectively.

In Chapter II, to establish a therapeutic approach targeting the JAK-STAT signaling pathway, the radio-sensitizing effect of oclacitinib in canine tumors and the underlying mechanisms were assessed in HMPOS and CMeC cell lines. Oclacitinib significantly enhanced the radio-sensitivity of tumor cells both *in vitro* and *in vivo*. In cells treated with X-irradiation exposure, STAT3 expression was significantly activated in a dose- and time-dependent manner, which was effectively suppressed by oclacitinib. Oclacitinib significantly enhanced radiation-induced apoptosis by inhibiting the expression of anti-apoptosis genes (*survivin*, *Bcl-x*$_L$, and *MCL1*) and Poly (ADP-ribose) polymerase (PARP) protein in HMPOS. Additionally, oclacitinib significantly inhibited the transcription of cell-cycle regulating genes (*CCND1*, *Cyclin-dependent kinase 4* and *6*) and arrested cell cycle progression from the G1 phase to subsequent phases. These results indicated that oclacitinib facilitated radio-sensitivity by triggering apoptosis and impeding cell cycle progression via STAT3 inhibition in canine tumor cell lines. This study suggested the clinical therapeutic potential of oclacitinib in combination with radiation therapy, aiming to enhance treatment efficacy and outcomes in dogs with tumors.

In conclusion, the regulatory mechanisms of PD-L1 expression on canine tumors

were elucidated. The JAK-STAT signaling pathway could play a pivotal role in the regulation of not only PD-L1 upregulation induced by IFN-γ but also the radio-sensitivity of canine tumors. In addition, oclacitinib targeting STAT3 was shown to be effective as a radio-sensitizer in canine tumors.